Elsevier Editorial System(tm) for Catena
Manuscript Draft

Manuscript Number: CATENA4977R2

Title: Post-fire erosion response in a watershed mantled by volcaniclastic deposits, Sarno Mountains, Southern Italy

Article Type: Research Paper

Keywords: wildfire; rainstorm; post-fire erosion response; soil loss; Sarno Mountains

Corresponding Author: Dr. GIUSEPPE ESPOSITO, M.D.

Corresponding Author's Institution: Consiglio Nazionale delle Ricerche - Istituto per l'Ambiente Marino Costiero

First Author: GIUSEPPE ESPOSITO, M.D.

Order of Authors: GIUSEPPE ESPOSITO, M.D.; FABIO MATANO, M.D.; FLAVIA MOLISSO, M.D.; GIOVANNA RUOPPOLO, PhD; ALMERINDA DI BENEDETTO, PhD; MARCO SACCHI, PhD

Abstract: In this study we document a post-fire erosion response to a short-lived, intense rainstorm occurred on 6 September, 2012 in the Sant'Angelo creek watershed, Sarno Mountains, Southern Italy. The rainstorm occurred one month after a wildfire that burned about 11 ha of the steep watershed (55 ha), almost entirely mantled by volcaniclastic deposits. The research was based on fieldwork and laboratory analysis addressed to the understanding of the geomorphic effects of the wildfire and their impact on erosional and depositional processes triggered by subsequent rainstorms. Field evidence indicates that a series of overland flows caused significant runoff and sediment yields along the hillslope and accumulation of hyperconcentrated flow deposits in a concrete channel occluded by a sealed culvert at the outlet of the watershed. The results of geomorphological and sedimentological analysis suggest that the occurrence of volcaniclastic covers mantling the slopes likely favored accelerated soil erosion, especially where vegetation and litter had been removed by the fire. Chemical analysis on sediment samples, revealed the occurrence of iron oxides that enhanced soil water repellency conditions over wide areas of the burned watershed compared to the unburned areas. Quantitative analysis of sediment budgets showed that the rainfall-induced erosion response at Sant'Angelo creek watershed resulted in a soil loss of 19.8 - 33.1 tons ha-1 over burned areas. Post-fire erosion response following severe rainstorms needs to be considered in the spectrum of natural hazards associated with the geomorphological evolution of mountainous landscapes mantled by volcaniclastic deposits.

Post-fire erosion response in a watershed mantled by volcaniclastic deposits, Sarno Mountains, Southern Italy

Giuseppe Esposito[a], Fabio Matano[a], Flavia Molisso[a], Giovanna Ruoppolo[b], Almerinda Di Benedetto[c], Marco Sacchi[a]

[a] Consiglio Nazionale delle Ricerche - Istituto per l'Ambiente Marino Costiero (CNR-IAMC), Calata Porta di Massa - Porto di Napoli, 80133 Napoli, Italy

[b] Consiglio Nazionale delle Ricerche - Istituto di Ricerche sulla Combustione (CNR-IRC), Piazzale V. Tecchio 80, 80125 Napoli, Italy

[c] Dipartimento di Ingegneria Chimica, dei Materiali e della Produzione Industriale, Università di Napoli Federico II, Piazzale V. Tecchio 80, 80125 Napoli, Italy

Corresponding author: Giuseppe Esposito, CNR-IAMC, Calata Porta di Massa - Porto di Napoli, 80133 Napoli, e-mail: giuseppe.esposito@iamc.cnr.it, tel.: +39 0815423834

Abstract

In this study we document a post-fire erosion response to a short-lived, intense rainstorm occurred on 6 September, 2012 in the Sant'Angelo creek watershed, Sarno Mountains, Southern Italy. The rainstorm occurred one month after a wildfire that burned about 11 ha of the steep watershed (55 ha), almost entirely mantled by volcaniclastic deposits. The research was based on fieldwork and laboratory analysis addressed to the understanding of the geomorphic effects of the wildfire and their impact on erosional and depositional processes triggered by subsequent rainstorms. Field evidence indicates that a series of overland flows caused significant runoff and sediment yields along the hillslope and accumulation of hyperconcentrated flow deposits in a concrete channel occluded by a sealed culvert at the outlet of the watershed. The results of geomorphological and sedimentological analysis suggest that the occurrence of volcaniclastic covers mantling the slopes likely favored accelerated soil erosion, especially where vegetation and litter had been removed by the fire. Chemical analysis on sediment samples, revealed the occurrence of iron oxides that enhanced soil water repellency conditions over wide areas of the burned watershed compared to the unburned areas.

Quantitative analysis of sediment budgets showed that the rainfall-induced erosion response at Sant'Angelo creek watershed resulted in a soil loss of 19.8 - 33.1 tons ha^{-1} over burned areas. Post-fire erosion response following severe rainstorms needs to be considered in the spectrum of natural hazards associated with the geomorphological evolution of mountainous landscapes mantled by volcaniclastic deposits.

Keywords: wildfire; rainstorm; post-fire erosion response; soil loss; Sarno Mountains.

1 Introduction

During the last decade, the role of wildfires as geomorphic agent has been widely recognized by the scientific community (e.g. ~~Shakesby and Doerr, 2006~~ Moody et al., 2013). Direct effects of wildfires on soil and vegetation (e.g. Certini, 2005; Shakesby and Doerr, 2006; Jordàn et al., 2013) may enhance erosion through sheetwash and rilling processes, often resulting in large mass movements (Swanson, 1981; Cannon et al., 1998; Wondzell and King, 2003; Nyman et al., 2011; Moody et al., 2013; Riley et al., 2013; Santi et al., 2013). Post-fire erosion responses may have a variety of impacts on landscapes. For instance, they can dominate the long-term sediment yield in a given area, until the geomorphic system returns to the typical conditions of unburnt terrain (Swanson, 1981; Prosser and Williams, 1998; Shakesby, 2011). Moreover, they represent a severe risk for human life, where houses and other infrastructures occur (Cannon and DeGraff, 2009; Nyman et al., 2011). Post-fire catastrophic floods and deadly debris or sediment-laden flows have been reported from several areas of Canada, western United States and southeastern Australia (e.g. Moody et al., 2013; Kean et al., 2011; VanDine et al., 2005; ~~Shakesby et al., 2003~~ Nyman, 2013). In the Mediterranean region, prevailingly moderate fire-related erosional events have been documented. However, as pointed out by Parise and Cannon (2008), most of research works in this area have dealt with experimental plots (e.g. Rosso et al., 2007) rather than analysis of post-wildfire landslides and erosional events. Case studies reported for Mediterranean region have mostly focused on Spain and Portugal (e.g. Lorente et al., 2002, 2003; Beguería, 2006; García-Ruiz et al., 2010, 2013; Lourenço et al., 2012) and fewer on the central countries, like in Italy and Greece (e.g. De vita et al., 1994; Tiranti et al., 2006; Calcaterra et al., 2007; Stefanidis et al., 2002; Blake et al., 2010).

The majority of the Mediterranean study areas are characterized by ~~the occurrence of~~ thin, stony soils, where surface erosion after wildfires is supply-limited with erosion rates ranging between 0.016 and 13.1 t ha^{-1} y^{-1} (Shakesby, 2011). A notable exception is represented by the volcanic areas of southern Italy, where local abundance of fine-grained, loose volcaniclastic material lying on steep volcanic and/or calcareous slopes may be observed (De Vita et al., 2006; Matano et al., 2016). Such material is often associated with andosols (WRB, 2006) characterized by relatively low cohesion under dry conditions (Maeda et al., 1977; Warkentin, 1984) and high erodibility when slope-stabilizing vegetation is absent (Rodriguez et al., 2002). The occurrence of wildfires in volcaniclastic settings is often reported, in fact, as a condition that enhances the probability of massive sediment-laden flows, as observed by Meyer and Wells (1997) in the Yellowstone National Park (U.S.A) and by Neris et al. (2016) in the Canary Islands (Spain). Nevertheless, according to Neris et al. (2016), hydrological and erosional response of this terrain type in the post-fire period has received little attention by the scientific community.

A distinctive feature of several regions of the central Mediterranean area is the local abundance of sediment-supplying soils occurring in steep slopes characterized by a plenty of easily flammable shrubs and forests. Such increase in the natural fuel load can be enhanced by inappropriate land use and/or land abandonment and afforestation with highly flammable species (Shakesby, 2011). Due to the combination of these factors with a likely increase in the frequency of extreme climatic events through time (Arca et al., 2010; Moriondo et al., 2006), future wildfire activity is expected to increase in the overall Mediterranean area.

In this study we document a post-fire erosion response to a short-duration, high-intensity rainstorm that occurred in the Sant'Angelo creek watershed, Sarno Mountain Range, southern Italy (Fig. 1). This area, characterized by a Mesozoic carbonate bedrock covered

by pyroclastic deposits and andosols, was partially burned on 4 August, 2012 (Esposito et al., 2013) and hit by a first rainstorm on 6 September, 2012.

The aims of this study are: (i) to improve knowledge about fire effects and related soil erosion processes in steep slopes covered by volcanic soils; (ii) to highlight that high amount of soil loss can occur in such contexts; (iii) to give a valid contribution towards the documentation of post-fire erosion responses occurring in the central Mediterranean area.

The research work was based on a multidisciplinary approach integrating fieldwork with chemical, mineralogical and grain size analysis conducted on soil samples collected in the study area. Similar approach was adopted in other erosional contexts of southern Italy (e.g. Summa et al., 2007; De Santis et al., 2010), demonstrating to be very suitable to investigate the effects and causes of erosion. Laboratory and field data were also used to quantify soil loss at the watershed scale.

2 The Sant'Angelo Creek watershed

2.1 Geological background

The Sant'Angelo Creek watershed is located in the Sarno Mountain Range, along the southern slope of Mt. Torrenone, about 3 km east of the town of Sarno (Fig. 1). The ridge is mainly formed by bedded Mesozoic carbonates (Di Nocera et al., 2011) and since the Late Quaternary it has been repeatedly mantled by pyroclastic airfall deposits, as a result of explosive activity of the Somma-Vesuvius (Rolandi et al., 1998) and Campi Flegrei (Orsi et al., 1996) volcanic districts (Fig. 1).

At the Sant'Angelo Creek watershed, the thickness of the volcaniclastic cover may vary significantly in different areas (Fig. 2), and it reaches a maximum of 5 m (De Vita et al., 2006; Autorità di Bacino del Sarno, 2011). However, slope-mantling deposits may be locally much thinner due to previous erosion and/or recent landslides. Figure 2 reports the

areal distribution of the varying thickness of volcaniclastic deposits that have been grouped into three classes (0,.1-0,.5 m; 0,.5-2,.0 m; 2,.0-5,.0 m), whereas carbonate scarps are referred to as exposed bedrock. The map indicates that in the burned area, the thickness of the pyroclastic cover mostly ranges from 0,5 m to 2,0 m. These volcaniclastic deposits are typically interbedded with a series of soil horizons classified as andosols (WRB, 2006), and characterized by a high content of glass and amorphous colloidal materials, including allophane and imogolite, and andic features ranging from high (Alo+0,5Feo>2%) to moderate (Alo+0,5Feo:1-2%) (Terribile et al., 2007).

2.2 Geomorphological setting

The morphology of the Sarno Mts. is marked by several tectonic lineaments (i.e. fault slopes) and carbonate scarps, along with gullies and karstic features with high gradients. Gullies are incised up to 30 m, and extend downslope from the ridge crest. Slope profiles are marked by a series of narrow scarps that may be followed laterally up to a few hundred meters. The scarps display heights ranging from 1-2 m to 10-15 m and typically correspond to erosion profiles of thick carbonate beds. Morphometric parameters of the Sant'Angelo creek watershed are summarized in Table 1, and a slope map of the watershed is showed in Fig. 2. Hillslopes are characterized by an average slope angle of about 35°. A marked decrease in the slope angles from 23° to 11° occurs along the channel slope at the outlet of the watershed.

The recent geomorphological evolution of the mountain range has been characterized by areal erosion along hillslopes with poor or absent vegetation, as well as by linear erosion along major valley axes. The most common instability processes in the study area are represented by rock falls affecting fractured carbonate scarps, and shallow landslides often involving the volcaniclastic covers. The Sarno Mountain Range area was also hit by a series of landslides evolving in downstream debris flows that occurred on 4-5 may 1998,

after a period of prolonged rainfall (120 mm of cumulated rainfall in 48 hours). The event caused 137 deaths in the town of Sarno (Cascini et al., 2008), and involved the volcaniclastic deposits and soils covering the carbonate slopes (Guadagno et al., 2005; De Vita et al., 2013). The slope instability, in this case, was mostly due to deterioration of mechanical properties of the volcaniclastic covers, as a consequence of the concentrated rainfalls and of the specific hydrological and geotechnical conditions (Cascini et al, 2003, 2013), which is substantially different from the post-fire erosional phenomena discussed in this work.

2.3 Meteo-climatic factors

The Sarno region is characterized by a typical Mediterranean climatic regime with hot, dry summers and moderately cool, rainy winters (Ducci and Tranfaglia, 2008). The annual average precipitation of this inner sector of the Apennines is in the order of 1000 mm/year at lower altitudes and 1400-1500 mm/year over summit areas.

In this part of the Mediterranean region, the major rainstorms following the peak summer period are caused by the Tropical-Like Cyclones (TLC), most of which occur between August and November (Tranfaglia and Braca, 2004; De Luca et al., 2010). Rainfalls from TLC are typically very intense and generally concentrated over small areas. Such meteorological systems, together with frontal storms and isolated convective cells, are able to trigger significant landslide phenomena, flash floods and debris flows (De Vita et al., 1994; Esposito et al., 2004; Esposito et al., 2015; Calcaterra et al., 2007; Porfido et al., 2009; Ciervo et al., 2012; Santo et al., 2012).

2.4 Fire regime

As in other Mediterranean countries, the occurrence of wildfires in Italy is concentrated during the hot and dry summer months, between July and September. ~~Here, the average~~

~~of the 40-year time series (1970-2010) is of about 9000 fires per year with an average burnt area of 105000 ha/yr (JRC, 2015).~~ The Italian territory extends over an area of 30.134 x 10^6 ha and, according to the State Forestry Corps (JRC, 2015), 8700 fires per year averaged in the period 1970-2015, burning about 100000 ha/yr. The Sant'Angelo creek fire is one of the 8252 fires that burned 130814 ha through the country in 2012. According to the State Forestry Corps, none of these events was related to natural causes, thus pointing at human responsibility in the ignition of many fires (JRC, 2013). Campania (Fig. 1) is one of the Italian regions most affected by fires. According to the Regional Department of Agriculture (2013), during 1991-2013, 60612 fires (average = 2635) burned a total surface of 161680 ha (average = 7030 ha). A remarkable number of these events affected the woodlands of the Sarno Mountains. In this area, in fact, 135 documented fires occurred in the period 2005-2015. The total burnt surface was 1118 ha, with an average fire size of 8 ha that is little less than the estimated average of 12 ha for Italy (JRC, 2015). In 2012, in addition to the Sant'Angelo creek fire, other 28 events hit the Sarno Mountain Range, causing a total burnt surface of about 220 ha.

3 Materials and methods

This research was based on integration of: a) geological and geomorphological data and soil burn severity assessment carried out at Sant'Angelo creek watershed during fieldwork; b) rainfall time series relevant to the analysis of the 6 September, 2012 meteorological event and c) sedimentological and chemical analysis of soil and sediment samples collected from the study area. Analysis of data included interpretation of geomorphic processes that developed along Sant'Angelo creek watershed and computation of erosion/deposition volumes of sediments involved in the post-fire response.

3.1 Analysis of geological and morphological data

Analysis of geological and morphological data of Sant'Angelo creek watershed was conducted through spatial analyst tools of ArcGIS 10.3^{TM}. As input data, we used a digital tridimensional model (DTM) of the watershed with a cell size of 5 m, and soil thickness data (Autorità di Bacino del Sarno, 2011). Data analysis allowed for extrapolation of morphometric properties of the study watershed and the construction of a thickness map of the pyroclastic covers. Results of this analysis are summarized in Table 1 and Figure 2.

3.2 Rainfall data

We analyzed data collected from three rain gauges located near the study area (Fig. 1). The most representative among these is the "Cetronico" rain gauge, located at a distance of 4.5 km to the east, along the same drainage divide with respect to the study area. All rainfall time series have been recorded at a sampling rate of 10 minutes. Relevant parameters derived from data acquired by the "Cetronico" rain gauge during the 6 September rainfall include: a) daily cumulative rainfall depth and 10-minute peak intensity (I_{10}); b) 30-minute rainfall intensity (I_{30}); c) total storm rainfall and duration; d) cumulative rainfall intensity and e) depth profiles. For the two other rain gauges only the total storm rainfall, duration, I_{10} and I_{30} are reported for comparisons.

3.3 Fieldwork data

The field survey started the day after the erosion response and involved both the study watershed and neighboring areas in order to verify the areal extension of erosional processes across the boundary between burned and unburned areas.

Qualitative metrics suggested by Parsons et al. (2010) were used to assess soil burn severity, which require evaluation of vegetation condition, soil water repellency, surface color and root condition. The persistency of soil water repellency was detected by in situ

Water Drop Penetration Time (WDPT) tests, following the method of DeBano (1981). In all sites, five pits were carried out and, in each of them, WDPT tests were performed ~~at the same depth~~ from the soil surface until a depth of 10 cm, with a step of 1 cm ~~for each pit~~. The median time between the five replications was used as the WDPT for ~~that~~ each depth. The results of soil burn severity assessment were summarized into two classes and then mapped in a soil burn severity map.

3.4 Sedimentological, chemical and mineralogical analyses

Laboratory analysis was conducted on samples collected from the areas characterized by high soil burn severity (B1 and B2) as well as from the outside of the burned area (NB1 and NB2) (Fig. 3). All samples ~~are~~ were representative of the bulk of the uppermost soil horizon from the surface down to a depth of ca.10 cm.

Soil samples were processed for grain size, chemical and mineralogical analysis (e.g. Summa et al., 2007). The results of laboratory analyses on these samples have provided relevant information to identify physical or chemical alteration of soils induced by fire that likely controlled the triggering mechanisms of erosion processes.

Two additional sediment samples (D1 and D2) were collected respectively from the tail and the front of a deposit observed after the 6 September 2012 rainstorm and trapped within the concrete channel at the outlet of the watershed (Fig. 3). For all samples ca. 300 g of material ~~have been~~ was collected.

Both sediment and soil samples were processed for grain size analysis, estimation of organic matter and water content, and specific gravity. The nature and percentage occurrence of constituents was determined using a Leica Zoom 2000 stereo microscope. The distribution of grain size fraction > 0.0125 mm was determined by sieve analysis, whereas the fraction < 0.0125 mm was analyzed by laser diffractometry (Sympatec). Grain

size statistical parameters including mean particle size, sorting, skewness and kurtosis have been calculated following the classic graphical method of Folk and Ward (1957).

The organic matter content of samples (SOM) was estimated following the LOI (Loss on Ignition) procedure suggested by Robertson (2011). The water content was evaluated by the gravimetric method. Specific gravity was calculated following the ASTM D-854 (2010) and the soil color was determined using a Munsell Soil Color Charts (1994).

Soil samples were also processed for the determination of major physical properties and chemical composition. An inorganic elemental analysis was conducted by inductively coupled plasma mass spectrometry (ICP-MS), using an Agilent 7500CE instrument after dissolving the fuel samples by means of microwave-assisted acid digestion, according to US-EPA 3051 and 3052. The soil modification after the fire was evaluated by measuring moisture, volatile, fixed carbon and ash content using a TGA 701 LECO thermo-gravimetric analyzer, according to the ASTM D-5142 standards.

Soil samples were processed for X-ray diffraction (XRD) using a PW 1100 Philips diffractometer in order to analyze the crystalline species. The obtained spectra were interpreted using the WWW-MINCRYST: Crystallographic and Crystallochemical Database for Minerals and their Structural Analogues. The morphology of materials was investigated with a FEI Inspect S SEM microscope.

3.5 Sediment erosion and deposition budgets

The post-fire erosion response that occurred on September 2012 at the Sant'Angelo creek watershed produced a massive deposit at the outlet of the watershed that was trapped in an artificial channel closed by a blocked culvert. In this case, the sealed channel acted as a watershed-scale sediment trap (Wells and Wohlgemuth, 1987; Robichaud and Brown,

2002; Morris et al., 2011) allowing for a computation of volume and weight of trapped sediments and a reliable estimate of the soil loss per unit area along the burned hillslope.

In order to estimate the total volume and weight of the soil mobilized by erosional processes along the hillslope and compare it with the weight of the deposits that have been found both within the artificial channel and along the slopes, two metrics were collected during the fieldwork: 1) thickness of eroded soil around the tree bases and 2) thickness of eroded soil by rills or rill depth (see section 4.3.1). These data were interpolated in ArcGis 10.3^{TM} software, in order to identify and map the areas characterized by the mobilized amounts of soil and their volumes. The weight corresponding to all measured volumes were calculated by using specific gravity derived from the study soil samples.

4 Data analysis and results

4.1 Soil burn severity

The fieldwork conducted in this study was specifically addressed to verify the occurrence of fire effects on vegetation and soil properties and eventually evaluate their spatial variability.

During the survey, we have observed that in some areas the crowns of oak trees were not completely leafless, the scorched leaves on trees had a light brown color and branches were only partially scorched. The surficial color was brown and a number of smaller roots near surface were slightly charred. Moreover, WDPT data, classified according with Bisdom et al. (1993), showed a slight water repellency characterized by infiltration times of 2-45 seconds (Table 2).

In other areas, there was evidence that some oak trees were bent by the winds during the fire and no leaves on their fully charred branches were detected. A black charred ground

surface was common and both small and larger roots were entirely charred near the surface, where a ca. 10 cm thick layer of litter, duff and bushes was destroyed by the flames. In these areas, WDPT tests revealed severe water repellency reflected by infiltration times also higher than half an hour (Table 2). Furthermore, rock fragments spalled during the fire were also found at the base of some charred carbonate outcrops. Following the suggestion of Parsons et al. (2010), these effects were used to discriminate among different soil burn severity classes. The soil burn severity map represented in Fig. 3 illustrates the extent and the various degrees of severity burned areas. Particularly, the map shows that the area characterized by high soil burn severity represents 65% of the 11 ha total burned surface, whereas the area corresponding to moderate soil burn severity, represents the 35% of the surface. The figure also indicates the location of soil and sediment sampling sites, WDPT test sites, and the path of the debris flow that struck the area of Sarno in 1998.

4.2 Rainfall properties

The post-fire response discussed in this work was triggered by a rainstorm generated within the tail of a low-pressure vortex formed above the Tyrrhenian Sea, off the Italian west coast (Weather forecast bulletin emitted by the Regional Civil Protection on 5 September, 2012). The storm had a radius of ca. 5 km and it was recorded by all the three rain gauges available for the study area (Table 3).

Particularly, the daily rainfall data of Cetronico gauge indicate that the precipitation over Sant'Angelo Creek watershed on 6 September, 2012 was characterized by both the highest 10-minute rainfall intensities and rain depths after the fire (Fig. 4). The rain gauge, recorded a total storm rainfall of 23.8 mm between 04:50 and 06:30 of that day. Within this time interval, 15.4 mm of rainfall occurred in the first 30 minutes (between 4:50 and 5:20),

with a 30-minute peak rainfall intensity (I_{30}) of 30.8 mm/h (Fig. 5). The 10-minute peak storm intensity (I_{10}) of 37.2 mm/h was reached between 5:10 and 5:20.

The inset of Fig. 5 shows that the rainfall intensity profile (black line) of the storm is characterized by a rapid rise with a peak followed by a relatively slow decline. The cumulative rainfall depth profile (gray line) also shows an initial rapid rise followed by a slower increase, thus confirming the character of short-duration, high-intensity convective of the storm.

4.3 Field indicators of post-fire geomorphic processes

4.3.1 Indicators of erosional processes

Several field indicators of erosional and depositional processes were identified during the ~~filed~~ field survey. Evidence of recent instability ~~have been~~ were not observed outside the burned parts of the watershed, where the vegetation cover is composed of 10 cm-thick litter, oak trees and the typical Mediterranean scrub (Fig. 6). Moreover, we did not observe any evidence of flow processes or deposits at the outlet of the nearby unburned watersheds during the survey.

Evidences of recent erosional processes detected on the slopes are summarized below.

1) Patches of crusted soil ~~have been~~ were identified locally. They are characterized by lighter color and higher compaction with respect to the adjacent surrounding areas. WDPT tests performed on ~~their~~ the surface consistently revealed a lack of infiltration capacity for an average thickness of 3 cm. The extension of individual patches is in the order of a few square decimeters.
2) Along the main runoff path, some aligned trees characterized by light annular bands at their base ~~have been~~ were detected (Fig. 7A). These bands correspond to parts of the bark that were covered by soil during wildfire, and ~~become~~ became visible

after post-fire erosion processes acted along the burned hillslope. The bands displayed a height of 2 - 8 cm and were often associated with bared roots (Fig. 7B).

3) A dozen of rill networks were also found in the burned area. Specifically, they were located where the fire burned with high soil burn severity, along the lower sector of slopes characterized by gradients of ca. 35° (Fig. 8). All networks appeared to be interrupted at slope breaks. Rills had a maximum length of ca. 10 m and a depth in the order of 10 - 20 cm. Individual rill scours had a width of 10 - 20 cm and no levees were detected along their margins.

Field data, including the height of the light bands at the base of the trees, and rill depth along burned slopes, suggest that the total volume of soil eroded along the burned hillslope was ca. 186 m^3. By considering a specific gravity of 2.2 g/cm^3 and a water content of 11.5 % for burned soils (Table 4), the resulting dry weight of the eroded material is ca. 364 tons.

4.3.2 Indicators of depositional processes

Several indicators of depositional processes were found both at the watershed outlet and along the burned slopes. The deposit found in the artificial channel at the outlet of the watershed (Fig. 9) is represented by mineral soil particles, ash, and charred plant remains. The concrete structure was built after the Sarno 1998 catastrophic landslide event, in order to funnel possible future debris flows into large storage basins downstream, and remained empty until the 6 September, 2012 rainstorm (see Google Earth historical images captured on 6/1/2010 and 7/14/2012 - 40°48'44.83"N, 14°39'40.28"E).

Field investigation showed that sediment and debris accumulation along the artificial channel was partly induced by the lack of maintenance of the culvert, with consequent obstruction of the hydraulic section, that caused a damming effect at the base of the channel. Traces of mud (Fig. 9) and splash marks were detected on the concrete banks.

The volume of flow deposit accumulated into the channel was estimated in ca. 175 m^3. Considering a specific gravity of 2.15 g/cm^3 and an average water content of 42 % (Table 4), the resulting dry weight of the deposit is ca. 218 tons.

Significant accumulation of sediments was found locally over the slopes, either behind the base of larger living trunks (Fig. 10), or trapped by the damming caused by charred branches and trunks intercepting runoff. Furthermore, patches of liquefied soil were found over carbonate scarps, locally filling-up the rough morphology. At least twenty areas of sediment and soil accumulation have been detected along the slope, with a cumulative volume of material of ca. 55 m^3, corresponding to an estimated total dry weight of ca. 88 tons of deposits.

4.4 Sedimentological characterization

Sedimentological analysis showed that both burned (B1, B2) and unburned (NB1, NB2) soil samples can be classified as gravelly muddy sand (Fig. 11) according to the classification system proposed by Folk (1974). This is also reflected by the similarity of grain size statistical parameters, soil organic matter and specific gravity reported in Table 4. Microscopic analysis showed that all samples had a relatively high volcaniclastic fraction content (70-100 %) and a low content of plant remains (0-30 %).

The sediment samples collected into the channel correspond to muddy sandy gravel (D1) and gravelly mud (D2) (Fig. 11). D1 is very poorly sorted (σ_G = 2.61) whereas D2 is poorly sorted (σ_G = 1.79). In terms of composition, sample D1 mostly consist~~s~~ of charred coarse-grained pyroclastic deposits with rare limestone rock fragments, whereas D2 ~~is~~ was represented by charred fine-grained volcaniclastics and plant remains (i.e. rootlets, leafs, charcoal and seed fragments). No unburned material was detected into the samples.

Both organic matter content and specific gravity showed significantly different values in the two samples (Table 4). The average water content was 42% whereas in the case of soil samples it was 11.5 %.

A comparison of grain size distribution of samples D1 and D2 with the facies distribution of a post-fire fan deposits (Meyer and Wells, 1997) is showed in Fig. 11. The curves of samples D1 and D2 fall within the hyperconcentrated flow and streamflow fields (Pierson and Costa, 1987), respectively. This evidence is consistent with a significant difference of sorting ($\sigma_{G\text{-}D1}$ = 2.61 - $\sigma_{G\text{-}D2}$ = 1.79) and with the traces of mud and splash marks detected on the concrete banks (Fig. 9). It also suggests the occurrence of low or no-internal strength turbulent flows characterized by high velocity.

4.5 Chemical/physical and mineralogical characterization

The results of the chemical/physical characterization of soil samples are summarized in Fig. 12 and Table 5 that shows the results of ICP analysis in terms of the concentration of major elements within the samples. The most abundant element is Aluminum (Si is not detected by ICP) followed by K, Ca, Fe, Mg and Na.

It is worth noting that the ICP analysis ~~displayed~~ displays no significant difference between the concentration of the main species of the burned (B) and unburned (NB) soil samples. This suggest that the phenomena occurring during the fire did not alter the inorganic material content. Consequently, only a rearrangement of the inorganic element can be hypothesized. Such results are in agreement with the results of SOM analysis and are also confirmed by the proximate analysis of all the samples given in Table 6, which shows that the content in volatiles is not affected by the exposition to the fire.

The results of the X-ray diffraction (XRD) analysis are shown in Fig. 13. The analysis was performed two times (Batch I, Batch II) for each soil sample in order to assess also the

homogeneity of the material. All the XRD spectra show signals (in the range 20-30 of 2σ angle) related to silicate species and more specifically to phyllosilicates and tectosilicates. In the burned sample, XRD signals at higher angle associated to the occurrence of iron oxides like hematite (Fe_2O_3), magnetite (Fe_3O_4) and wustite (FeO) are present. The important role of both amorphous and crystalline Fe in stabilizing natural soil aggregates has been proved by many authors. In particular, Jozefaciuk and Czachor (2014) report that an increasing content of Fe causes a decrease in the water stability of small (ca. 1 mm) and large (ca. 1 cm) aggregates.

The morphology of materials was investigated with a FEI Inspect S SEM microscope. The image of the different samples under different magnitude are reported in Fig. 14. The SEM analysis performed on the NB1 and NB2 samples shows a layered structure composed of phyllosilicates and tectosilicates. The particles show a poor sphericity and roundness and a large size distribution. A comparison of the SEM images of burned and unburned samples suggests that the morphology and the degree of sphericity and roundness are unaffected by the fire.

5 Discussion

5.1 Post-fire geomorphic processes

Morphometric properties showed in Table 1 highlight the occurrence of steep slopes and moderate channel gradients in the Sant'Angelo creek watershed. As widely reported in the literature, steep morphologies may enhance fire intensity and spreading, and increase the potential for surface erosion and mass movements. Indeed the steep topographic conditions of the study area (average slope angle = 35°) may have exerted a significant control on both the soil burn severity and erosional processes.

The results of the fieldwork indicate that the Sant'Angelo creek fire burned 65% of the 11-ha affected area with high severity and 35% with moderate severity. The wildfire caused partial consumption of the tree canopy, shrubs, soil-mantling litter and duff, as well as modification of soil properties (i.e. water repellency). These effects may have been controlled not only by the steep topography but also by high availability of fuel (Fig. 6) and local weather conditions. For instance, a number of bent oak trees found in the burned area suggest, that strong winds occurred during the fire propagation.

Water repellency was investigated in the field through WDPT tests, and showed persistency ranging from slight to severe. The results of mineralogical analysis suggest that iron oxides, that occur in burned soil samples but are not present in the unburned soil samples, could have enhanced this behavior. Particularly, the occurrence of iron oxides indicates that the upper soil horizon underwent relatively high temperature (250 C) coupled with high oxygen and water content. It has been in fact demonstrated that in highly oxygenated conditions, with high partial pressure, the formation of iron oxides is significantly high (Bertrand et al, 2010).

New aggregates formed by clay, silt and sand particles bound by Fe oxides (Regelink et al., 2015) may lead to a decrease in the soil porosity, which in turn produces a decrease in the soil permeability. According with Gargiulo et al. (2013), iron oxides may cause a 50% reduction of porosity in soils characterized by significant sandy content and low shrinking-swelling capacity. Considering the results of chemical analysis, coupled with mineralogical and textural properties of the analyzed volcanic soils, we infer that a similar mechanism of increased water repellency conditions may have occurred during the Sant'Angelo creek fire. It cannot be excluded that micro-aggregates had formed as hydrophobic compounds generated in the plants litter and migrated downward in the soil along with water vapor and oxygen (DeBano, 2000). Comparison of SEM images with grain size and composition

1 does not indicate any significant structural difference between burned and unburned
2 samples. This would exclude other causes controlling the water repellency conditions.
3 The rainstorm that occurred in the study area about one month after the fire was
4 characterized by 30-minute peak rainfall intensity (I_{30}) of 30.8 mm/h, triggering a high-
5 magnitude erosion response. A series of indicators recognized during the field survey
6 allowed us to identify the post-fire geomorphic processes triggered by the rainstorm.

7 Several indicators highlight the occurrence of sheetwash erosion (Shakesby and Doerr,
8 2006) along the burned hillslope. Clear evidences are the light bands found at the base of
9 some trees (Fig. 7A), indicating the occurrence of overland flows which removed the loose,
10 friable, and burned mineral soil around the base of the trunks, with a progressive
11 entrainment of material downslope. Suspended sediments transported by overland flows
12 also included soil particles detached during the raindrops impact. As stated by McGuire et
13 al. (2016), steep burned areas characterized by sandy soils may be particularly
14 susceptible to the raindrop-driven detachment process, making the soil surface more
15 erodible and prone to flow-driven transport. Additional evidence of rainsplash detachment
16 is represented by local patches of soil crusts found on the burned slope (Farres, 1987; Le
17 Bissonnais et al.,1989; Mataix-Solera et al., 2011).

18 The local transition from diffusive erosion dominated by sheetwash to concentrated
19 erosion is testified by rill networks (Fig. 8). The occurrence of rills suggests that, localized
20 Hortonian infiltration-excess may have been a major hillslope-runoff-generating process
21 (e.g. DeBano, 2000). However, it cannot excluded that this process may have included
22 transition and/or switching between infiltration-excess and saturation-excess conditions.
23 It was not surprising to find rill networks in the burned area, given the high slope gradients
24 (Table 1) and soil burn severity conditions (Fig. 3). In fact, where volcaniclastic deposits
25 occur (e.g. Las Conchas wildfire, Pellettier and Orem, 2014), rilling can be the most

common form of hillslope erosion observed in areas characterized by moderate and high soil burn severity. ~~Meyer and Wells (1997) and Staley et al. (2014) also observed a consistent development of rill networks supplying material for runoff-generated debris flows in steep landscapes.~~

As detected during field survey, a part of the upper soil horizon including mineral soil particles, ash, charcoal, branches and leaves transported by overland flows was redistributed along the hillslope because of micro-topographic conditions. However, the massive deposit found into the artificial channel at the outlet of watershed (Fig. 9) suggests that ~~a significant part~~ about 60% of the mobilized sediments (i.e. 218 of 364 tons) traveled into the main drainage axis of the Sant'Angelo Creek watershed down to the concrete channel, as a gravity flow.

According to what has been observed by Keane et al. (2011) in southern California, we infer that the Sant'Angelo Creek flows possibly initiated shortly after the beginning of the rainfall event, when the estimated 30-minute rainfall intensity (I_{30}) exceeded the threshold value of 20 mm/h for 30 minutes proposed by Cannon et al. (2003 a, b). Decreasing intensity through time (Fig. 5) could have controlled the sediment-water mixture concentration (e.g. Keane et al. 2013). We infer that such variation may have implied transition from hyperconcentrated flow to streamflow (Pierson and Costa, 1987) corresponding to a decrease in the sediment transport capacity towards the final stage of the flow response. The overall grain size diversity between samples D1 and D2 (Fig. 11) may indicate such a tendency. Particularly, we suggest that hyperconcentrated flow deposits may be regarded as the result of massive deposition during the main flow event, whereas streamflow deposits may represent the product of the downstream deposition of flow tail, characterized by abundant fine-grained fraction (sample D2) and plant debris washed away from coarse material deposited upstream (sample D1). The occurrence of

similar facies association has been already reported in the literature for post-fire responses in other regions (Meyer and Wells 1997; Cannon et al., 1998; Kean et al., 2011), sometimes with specific reference to lahars in volcaniclastic settings (Scott, 1988; Pierson, 2005). According to Meyer and Wells (1997), burned slopes are broadly analogous to slopes mantled by loose volcaniclastic materials in terms of runoff potential and availability of fine sediment. In this study, due to the coupling of both factors (volcaniclastic materials and burned slope), we suggest that the post-fire flow processes here described could be regarded as of lahar-type.

The results discussed in this section highlight the importance of collecting post-fire field observations, especially in the central Mediterranean area where most of the available studies are based on simulated rainfall and/or experimental plots addressed to the modeling of post-fire erosion responses (e.g. Rulli et al., 2013, 2006; Vafeidis et al., 2007). Field data are indeed essential to understand mechanisms controlling the initiation and propagation of mass movements (e.g. Cannon et al., 2001; Nyman et al., 2011), and provide useful information to calibrate both models for predicting runoff-generated erosion (Nyman et al., 2015; Kean et al., 2013) and compile catalogues related to post-fire events (Gartner et al., 2005; Riley et al., 2013).

The limited number of post-fire erosion events documented in the study region makes somewhat problematic the understanding of the triggering factors or predisposing conditions controlling post-fire erosion responses. In volcaniclastic settings, not far from the study area, Calcaterra et al. (2007) and De Vita et al. (1994) documented that different post-fire geomorphic processes (e.g. landslides and debris flows) may occur in similar landscapes, also causing fatalities.

5.2 Post-fire soil loss

The soil erosion intensity map of Fig. 9 shows the areas involved by the post-fire response and the artificial channel at the outlet of the watershed. On the basis of the interpolation of fieldwork data, as a first step, we have inferred the volumes involved by erosion and subsequent depositional processes. Secondly, we have derived the soil loss per unit area at the watershed scale.

The balance between eroded and deposited sediments highlights a net excess of 58 tons of eroded material. This material was ostensibly redistributed along the hillslope and/or washed away from the channel by overland flows as suspended sediments. Since there was no significant evidence of erosion and instability processes in the unburned parts of the watershed, the burned sector can be regarded as the primary source area for the gravity flow deposits that accumulated in the concrete channel downstream.

Different estimates of the average post-fire soil loss can be obtained by dividing in turn the dry weight of channel deposits (218 tons), total deposited sediments (including hillslope and channel deposits, 306 tons) and eroded materials (364 tons) for the burned area (11 ha), resulting in a soil loss of 19.8, 27.8 and 33.1 tons ha^{-1}, respectively. This tendency to soil loss in the sediment budgets may be the result of larger scale entrapment of thin layers of material mobilized along the slopes, and/or by the dominance of hillslope processes over base of slope (channel) processes. Apparent soil loss in the system may also result from the occurrence of significant volumes of sediment or debris stored in the channel network, prior to the wildfire event.

The problem of soil loss during post-fire response events has been long debated in the literature. Shakesby (2011) reports values ranging between 0.016 and 13.1 tons ha^{-1} during the first year after wildfire for Mediterranean regions and 2.5 to 197 tons ha^{-1} in the USA and Australia. The case of Sant'Angelo Creek watershed seems in good agreement

with annual erosion data collected at the catchment scale of the Mediterranean area and with figures documented in other regions after specific events (e.g. Copeland, 1965; Shakesby and Doerr, 2006; Moody and Martin, 2009; Lavabre and Martin, 1997; Robichaud et al., 2013). For example, Robichaud et al. (2013) reported soil losses of 18.6 tons ha^{-1} and 24.4 tons ha^{-1} after two short-duration high-intensity rainstorms (10-min maximum rainfall intensity respectively of 52 mm/h and 65 mm/h) in a 4.6-ha watershed in Colorado. Similarly, Copeland (1965) reported a soil loss of 9.6 tons ha^{-1} in a 98-ha watershed, in Nevada, during a rainstorm that reached a 5-min maximum rainfall intensity of 234.7 mm/h.

The methodological approaches of various authors and the different size of the burned areas represents one of the main problems in the calculation of soil loss within burned landscapes (Shakesby and Doerr, 2006; Moody and Martin, 2009). In this study, the calculated soil loss seems to be consistent both with the abundance of highly erodible volcaniclastic soils mantling the carbonate slopes and with the moderate and high soil burn severity of the Sant'Angelo Creek watershed event.

The volcanic soils of study area, indeed, are very different from the typical thin and stony soils of the Mediterranean regions whose thickness is normally up to 35-50 cm (Shakesby, 2011). The soils involved by the Sant'Angelo creek fire are mainly 0.5 – 2.0 m thick (Fig. 2) and typically cohesionless (Damiano and Olivares, 2010). As a consequence, the shear strength of the topsoil horizons is significantly dependent by the occurrence of plant roots, as quantified by Nyman et al. (2013) for non-cohesive burned soils in Australia and United States.

Moreover, the role played by the vegetation is fundamental in reducing the kinetic energy of the raindrops and generating a mulch layer that prevents soil desiccation in low-rainfall periods. Therefore, we infer that in the study area, the burning of vegetation and litter

cover caused by the wildfire resulted in effective erosion and transportation of fine sediment along the slopes.

According to Shakesby (2011), fire severity represents a key factor in controlling the degree of post-fire erosion. The Sant'Angelo creek event was characterized by moderate and high soil burn severity (35% and 65% respectively). According to our interpretation the fire had caused a significant decrease in the aggregate stability within the topsoil that likely reduced the critical shear stress required for the initiation of erosional processes (Moody and Smith, 2005; Mataix-Solera et al., 2011). According to Nyman et al. (2013), high severity wildfires can produce a hit pulse penetrating deeper into the soil than low-severity wildfires, and this may increase the corresponding depth of non-cohesive layer.

Based on the above observations we suggest that these factors, combined with the morphology of Sant'Angelo creek watershed and the intensity of the rainstorm event discussed in this study, have produced significantly high erosion and large volumes of sediments transported by overland flows downstream.

6 Conclusions

The data presented in this study document cause - effect relationship between the Sant'Angelo Creek fire (~~6~~4 August, 2012) and the subsequent (6 September, 2012) post-fire erosion response. The event was triggered by a convective high-intensity and short-duration rainstorm that generated soil and sediment mass movements along the Sant'Angelo Creek watershed.

Erosion over the slopes was primarily driven by the entrainment of material due to runoff during post-fire erosion responses, and evolved with different magnitudes, mostly depending on slope morphology, vegetation cover and rain intensity. Quantitative analysis of sediment budgets showed that the Sant'Angelo Creek response caused a soil loss of about 19.8 to 33.1 tons ha^{-1} in the burned zone.

The results of this research suggest that wildfires can play a significant role in the geomorphological evolution of mountainous landscapes of the southern Apennines and similar contexts of the central Mediterranean area, especially when associated with heavy rainfall events. However, the lack of documented post-fire erosion responses, as well as inadequate knowledge about fire effects on volcanic soils of this geographic area, represent important issues. In order to better post-fire erosion mitigation strategies or emergency-response planning, future efforts to fill these research gaps are therefore essential.

Acknowledgements

This research work has been partly carried out during a CNR Short Term Mobility (STM) program conducted by G. Esposito at the USGS, Golden (CO), USA.

Thanks are due to S. Cannon, D. Staley, J. Coe, D. Martin, J. Moody and B. Ebel for fruitful discussions and precious comments on fire-related processes and to J. Kean for the review of an early version of the manuscript. Analyses on soil and rock samples were conducted with the precious support of M. Capodanno in the sedimentological laboratory of the IAMC-CNR Institute, Napoli.

We gratefully thank Luciano Cortese and Fernando Stanzione for SEM, XRD and ICP analyses. We also acknowledge the Civil Protection Department of Campania Region for allowing us access to rainfall data on the study area for the period August - September 2012 as well as the State Forestry Corps of Sarno for providing us information on wildfires in the study area, and Municipality of Sarno for providing us the DTM of the study area.

Financial support was provided by the Research Project PON-MONICA (contract n° PON01_01525) and the 2013 CNR STM Program.

References

Arca, B., Pellizzaro, G., Duce, P., 2010. Climate change impact on fire probability and severity in Mediterranean areas, in: Proceedings of the "VI International Conf. on Forest Fire Research", Coimbra, Portugal, 15-18 November 2010.

ASTM D-5142, 1996. Standard Test Methods for Proximate Analysis of the Analysis Sample of Coal and Coke by Instrumental Procedures. ASTM Book of Standards Vol. 05.05, West Conshohocken, PA.

ASTM Standard D-854, 2010. Specific Gravity of Soil Solid by Water Pycnometer. ASTM International West Conshohocken, PA.

Autorità di Bacino del Sarno, 2011. Piano Stralcio di Bacino per l'Assetto Idrogeologico – Carta degli spessori delle coperture piroclastiche in scala 1:5000, Napoli, Italy.

Beguería, S., 2006. Changes in land cover and shallow landslide activity: a case study in the Spanish Pyrenees. Geomorphology 74, 196–206.

Bertrand, N., Desgranges, C., Poquillon, D., Lafont, M.C., Monceau, D., 2010. Iron Oxidation at Low Temperature (260–500 C) in Air and the Effect of Water Vapor. Oxidation of Metals 73, 39–162.

Bisdom, E.B.A., Dekker, L.W., Schoute, J.F.T., 1993. Water repellency of sieve fractions from sandy soils and relationships with organic material and soil structure. Geoderma 56, 105-118.

Blake, W.H., Theocharopoulos, S.P., Skoulikidis, N., Clark, P., Tountas, P., Hartley, R., Amaxidis, Y., 2010. Wildfire impacts on hillslope sediment and phosphorus yields. Journal of Soils and Sediments 10, 671-682.

Calcaterra, D., Parise, M., Strumia, S., Mazzella, E., 2007. Relations between fire, vegetation and landslides in the heavily populated metropolitan area of Naples, Italy,

in: Proceedings 1st North American Landslides Conference, Vail, Colorado. AEG Special Publication 23, pp. 1448-1461.

Cannon, S.H., Bigio, E.R., Mine, E., 2001. A process for fire-related debris flow initiation, Cerro Grande fire, New Mexico. Catena 70, 396-409.

Cannon, S.H., DeGraff, J.D., 2009. The increasing wildfire and post-fire debris-flow threat in Western USA, and implications for consequences of climate change, in: Sassa K, Canuti P (eds) Landslides—disaster risk reduction. Springer, Berlin Heidelberg, pp. 177–190.

Cannon, S.H., Gartner, J.E., Holland-Sears, A., Thurston, B.M., Gleason, J.A., 2003a. Debris-flow response of basins burned by the 2002 Coal Seam and Missionary Ridge fires, Colorado, in: Boyer, D.D., Santi, P.M., Rogers, W.P. (Eds.), Engineering Geology in Colorado Contributions, Trends, and Case Histories. AEG Special Publication 15.

Cannon, S.H., Gartner, J.E., Parrett, C., Parise, M., 2003b. Wildfire-related debris flow generation through episodic progressive sediment bulking processes, western U.S.A, in: Rickenmann, D., Chen, C.L. (Eds.), Debris-Flow Hazards Mitigation: Mechanics, Prediction, and Assessment. Millpress, Rotterdam, in: Proceedings 3rd International DFHM Conference, Davos, Switzerland, pp. 71-82.

Cannon, S.H., Powers, P.S., Savage, Z., 1998. Fire-related debris flows on Storm King Mountain, Glenwood Springs, Colorado, USA. Environmental Geology 35, 210–218.

Cascini, L., Sorbino, G., Cuomo, S., 2003. Modelling of flowslides triggering in pyroclastic soils, in: Fasl Slope Movements Prediction and Prevention for Risk Mitigation, pp. 93-100. Bologna, PATRON. ISBN:8855526995

Cascini, L., Cuomo, S., Guida, D., 2008. Typical source areas of May 1998 flow-like mass movements in the Campania region, Southern Italy. Engineering Geology 96(3), 107-125.

Cascini, L., Sorbino, G., Cuomo, S., Ferlisi, S., 2013. Seasonal effects of rainfall on the shallow pyroclastic deposits of the Campania region (southern Italy). Landslides 11, 779-792.

Certini, G., 2005. Effects of fire on properties of forest soils: a review. Oecologia 143, 1–10.

Ciervo, F., Medina, V., Papa, M.N., Bateman, A., 2012. Reconstruction and numerical modelling of a flash flood event: Atrani 2010, In: Proceedings of the International workshop on flash flood and debris flow risk management in Mediterranean areas, Salerno, Italy, p. 21.

Copeland, O.L., 1965. Land use and ecological factors in relation to sediment yields, in: Proceedings of Federal Interagency Sedimentation Conference, 1963: U.S. Dept. Agriculture Misc. Pub. 970, pp. 72-84

Damiano, E., Olivares, L., 2010. The role of infiltration processes in steep slope stability of pyroclastic granular soils: Laboratory and numerical investigation. Natural Hazards 52, 329-350.

DeBano, L.F., 2000. The role of fire and soil heating on water repellency in wildland environments: a review. Journal of Hydrology 231–232, 195–206.

DeBano, L.F., 1981. Water repellent soils: a state of the art. USDA Forest Service General Technical Report PS W-46.

De Luca, C., Furcolo, P., Rossi, F., Villani, P., Vitolo, C., 2010. Extreme rainfall in the Mediterranean, in: Proceedings of the International Workshop on Advances in statistical hydrology, Taormina, Italy.

http://www.risorseidriche.dica.unict.it/Sito_STAHY2010_web/proceedings.htm (accessed 10.1.16).

De Santis, F., Giannossi, M.L., Medici, L., Summa, V., Tateo, F., 2010. Impact of physico-chemical soil properties on erosion features in the Aliano area (Southern Italy). Catena 81, 172-181.

De Vita, P., Napolitano, E., Godt, J., Baum, R., 2013. Deterministic estimation of hydrological thresholds for shallow landslide initiation and slope stability models: case study from the Somma-Vesuvius area of southern Italy. Landslides 10, 713-728.

De Vita, P., Celico, P., Siniscalchi, M., Panza, R., 2006. Distribution, hydrogeological features and landslide hazard of pyroclastic soils on carbonate slopes in the area surrounding Mount Somma-Vesuvius (Italy). Italian Journal of Engineering Geology and Environment 1, 75–98.

De Vita, P., Guadagno, C., Lanzara, R., Lombardi, G., Tarantino, E., Vallario, A., 1994. L'evento alluvionale del 20 agosto 1993 nei territori comunali di Solofra e Serino (Avellino - Campania), in: Atti VIII Congresso Nazionale Geologi, Roma, Italy, pp. 165-171.

Di Nocera, S., Matano, F., Pescatore, T., Pinto, F., Torre, M., 2011. Geological Characteristics of the External Sector of the Campania-Lucania Apennines in the CARG Maps. Rendiconti Online della Società Geologica Italiana 12, 39-43.

Ducci, D., Tranfaglia, G., 2008. The Effect of Climate Change on the Hydrogeological Resources in Campania Region (Italy), in: Dragoni, W., Sukhija, B.S. (Eds.), Climatic

changes and Groundwater. Geological Society, Special Publications 288, London, pp. 25-38.

Esposito, E., Porfido, S., Tranfaglia, G., Iaccarino, G., Esposito, G., Braca, G., 2004. Correlation between pluviometric data and sliding phenomena in Naples, Southern Italy. Atti dei convegni lincei - accademia nazionale dei lincei 181, 379-386.

Esposito, G., Esposito, E., Matano, F., Molisso, F., Porfido, S., Sacchi, M., 2013. Effects of a wildfire on rocks and soils in the Sarno Mountains, Campania, Southern Apennines. Rendiconti Online della Società Geologica Italiana 24, 119-121.

Esposito, G., Fortelli, A., Grimaldi, M.G., Matano, F., Sacchi, M., 2015. I fenomeni di flash flood nell'area costiera di Pozzuoli (Napoli, Italia): risultati preliminari sull'analisi dell'evento del 6 novembre 2011. Rendiconti Online della Società Geologica Italiana 34, 74-84.

Farres, PJ., 1987. The dynamics of rainsplash erosion and the role of soil aggregate stability. Catena 14, 119-130.

Folk, R.L., 1974. Petrology of Sedimentary Rocks. Hemphill Publishing Company, Austin, 182.

Folk, R.L., Ward, W.C., 1957. Brazos river bar: a study of significante of grain size parameters. Journal of Sedimentary Petrology 27, 3-26.

García-Ruiz, J.M., Arnáez, J., Gómez-Villar, A., Ortigosa, L., Lana-Renault, N., 2013. Fire-related debris flows in the Iberian Range, Spain. Geomorphology 196, 221-230.

García-Ruiz, J.M., Beguería, S., Alatorre, L.C., Puigdefábregas, J., 2010. Land cover changes and shallow landsliding in the Flysch Sector of the Spanish Pyrenees. Geomorphology 124, 250–259.

Gargiulo, L., Mele, G., Terribile, F., 2013. Image analysis and soil micromorphology applied to study physical mechanisms of soil pore development: An experiment using iron oxides and calcium carbonate. Geoderma 197-198, 151-160.

Gartner, J.E., Bigio, E.R., Cannon, S.H., 2005. Compilation of post wildfire runoff-event data from the Western United States. U.S. Geological Society Open-File Report 2004–1085. http://pubs.usgs.gov/of/2004/1085/ofr-04-1085.html (accessed 3.10.15).

Guadagno, F.M., Forte, R., Revellino, P., Fiorillo, F., Focareta, M., 2005. Some aspects of the initiation of debris avalanches in the Campania Region: The role of morphological slope discontinuities and the development of failure. Geomorphology 66, 237–254.

ISPRA (Istituto Superiore per la Protezione e la Ricerca Ambientale) – Servizio Geologico d'Italia, 1976. Geological map of Italy at 1:100,000 scale, Roma, Italy.

JRC - Joint Research Centre, 2015. Forest Fires in Europe, Middle East and North Africa 2014. http://forest.jrc.ec.europa.eu/effis/reports/annual-fire-reports/ (accessed 02.10.2016).

JRC - Joint Research Centre, 2013. Forest Fires in Europe, Middle East and North Africa 2012. http://forest.jrc.ec.europa.eu/effis/reports/annual-fire-reports/ (accessed 02.10.2016).

Jordàn, A., Zavala, L.M., Mataix-Solera, J., Doerr, S.H., 2013. Soil water repellency: Origin, assessment and geomorphological consequences. Catena 108, 1-5.

Jozefaciuk, G., Czachor, H., 2014. Impact of organic matter, iron oxides, alumina, silica and drying on mechanical and water stability of artificial soil aggregates: Assessment of new method to study water stability. Geoderma 221–222, 1–10.

Kean, J.W., McCoy, S.W., Tucker, G.E., Staley, D.M., Coe, J.A., 2013. Runoff-generated debris flows: Observations and modeling of surge initiation, magnitude, and frequency. Journal of Geophysical Research: Earth Surface 118, 2190-2207.

Kean, J.W., Staley, D.M., Cannon, S.H., 2011. In situ measurements of post-fire debris flows in southern California: Comparisons of the timing and magnitude of 24 debris-flow events with rainfall and soil moisture conditions. Journal of Geophysical Research 116, F04019.

Lavabre, J., Martin, C., 1997. Impact d'un incendie de forêt sur l'hydrologie et l'érosion hydrique d'un petit bassin versant méditerranéan. Human Impact on Erosion and Sedimentation, in: Proceedings of Rabat Symposium S6, April 1997, IAHS Publication 245, pp. 39-47.

Le Bissonnais, Y., Bruand, A., Jamagne, M., 1989. Laboratory experimental study of soil crusting: relation between aggregate breakdown mechanisms and crust structure. Catena 16, 377-392.

Lorente, A., Beguería, S., Bathurst, J.C., García-Ruiz, J.M., 2003. Debris flow characteristics and relationships in the Central Spanish Pyrenees. Natural Hazards and Earth System Sciences 3, 683–692.

Lorente, A., García-Ruiz, J.M., Beguería, S., Arnáez, J., 2002. Factors explaining the spatial distribution of hillslope debris flows. A case study in the Flysch Sector of the Central Spanish Pyrenees. Mountain Research and Development 22, 32–39.

Lourenço, L., Nunes, A.N., Bento-Gonçalves, A., Vieira, A., 2012. Soil erosion After Wildfires in Portugal: What Happens When Heavy Rainfall Event Occur?, in: Danilo Godone, Silvia Stanchi (Ed.), Research on Soil Erosion, InTech, ISBN: 978-953-51-0839-92.

Maeda, T., Takenaka, H., Warkentin, B.P., 1977. Physical properties of allophane soils. Advances in Agronomy 29, 229-264.

Mataix-Solera, J., Cerdà, A., Arcenegui, V., Jordán, A., Zavala, L.M., 2011. Fire effects on soil aggregation: a review. Earth-Science Reviews 109, 44-60.

Matano, F., De Chiara, G., Ferlisi, S., Cascini, L., 2016. Thickness of pyroclastic cover beds: the case study of Mount Albino (Campania region, southern Italy). Journal of Maps 12, 79-87. ~~http://www.tandfonline.com/doi/full/10.1080/17445647.2016.1158668 (accessed 02.10.2016)~~.

McGuire, L.A., Kean, J.W., Staley, D.M., Rengers, F.K., Wasklewicz, T.A., 2016. Constraining the relative importance of raindrop- and flow-driven sediment transport mechanisms in postwildfire environments and implications for recovery time scales, Journal of Geophysical Research: Earth Surface 121, 1-27.

Meyer, G.A., Wells, S.G., 1997. Fire-related sedimentation events on alluvial fans, Yellowstone National Park, U.S.A. Journal of Sedimentary Research 67, 776-79.

Moody, J.A., Shakesby, R.A., Robichaud, P.R., Cannon, S.H., Martin, D.A., 2013. Current research issues related to post-wildfire runoff and erosion processes. Earth-Science Reviews 122, 10-37.

Moody, J.A., Martin, D.A., 2009. Synthesis of sediment yields after wildland fire in different rainfall regimes in the western United States. International Journal of Wildland Fire 18, 96-115.

Moody, J.A., Smith, J.D., 2005. Critical shear stress for erosion of cohesive soils subjected to temperatures typical of wildfires. Journal of Geophysical Research 110, 1-13.

Moriondo, M., Good, P., Durao, R., Bindi, M., Giannakopoulos, C., Corte-Real, J., 2006. Potential impact of climate change on fire risk in the Mediterranean area. Climate Research 13, 85-95.

Morris, R., Buckman, S., Connelly, P., Dragovich, D., Ostendorf, B., Bradstock, R., 2011. The dirt on assessing post-fire erosion in the Mount Lofty Ranges: comparing methods, in: Proceedings of Bushfire CRC & AFAC 2011 Conference Science Day, Sydney, Australia, pp. 152-169.

Munsell Soil Color Charts., 1994. New Windson: Kollmorgen Instruments-Macbeth Division.

Neris, J., Santamarta, J.C., Doerr, S.H., Prieto, F., Agulló-Pérez, J., Garcìa-Villegas, P., 2016. Post-fire soil hydrology, water erosion and restoration strategies in Andosols: a review of evidence from the Canary Islands (Spain). iForest - Biogeosciences and Forestry (early view), e1-e10.

Nyman, P., 2013. Post-fire debris flows in southeast Australia: initiation, magnitude and landscape controls. PhD thesis, Melbourne School of Land and Environment, The University of Melbourne.

Nyman, P., Smith, H.G., Sherwin, C.B., Langhans, C., Lane, P.N.J., Sheridan, G.J., 2015. Predicting sediment delivery from debris flows after wildfire. Geomorphology 250, 173-186.

Nyman, P., Sheridan, G. J., Smith, H. G., Lane, P. N. J., 2011. Evidence of debris flow occurrence after wildfire in upland catchments of south-east Australia. Geomorphology 125, 383-401.

Nyman, P., Sheridan, G.J., Moody, J.A., Smith, H.G., Noske, P.J., Lane, P.N.J., 2013. Sediment availability on burned hillslopes. Journal of Geophysical Research: Earth Surface 118, 2451-2467.

Orsi, G., De Vita, S., Di Vito, M., 1996. The restless, resurgent Campi Flegrei Nested Caldera (Italy): Constraints on its evolution and configuration. Journal of Volcanology and Geothermal Research 74, 179–214.

Parise, M., Cannon, S., 2008. The effects of wildfires on erosion and debris-flow generation in Mediterranean climatic areas: a first database, in: Proceedings of 1st World Landslide Forum, Tokyo, Japan, pp. 465-468.

Parsons, A., Robichaud, P.R., Lewis, S.A., Napper, C., Clark, J.T., 2010. Field guide for mapping post-fire soil burn severity. USDA Forest Service, Fort Collins, Colorado, General Technical Report RMRS-GTR-243.

Pelletier, J.D., Orem, C.A., 2014. How do sediment yields from post-wildfire debris-laden flows depend on terrain slope, soil burn severity class, and drainage basin area? Insights from airborne-LiDAR change detection. Earth Surface Processes and Landforms 39, 1822-1832.

Pierson, T.C., 2005. Hyperconcentrated flow-transitional process between water flow and debris flow, in: Jakob, M., Hungr, O. (Eds.), Debris-flow Hazards and Related Phenomena. Springer/Praxis, Chichester (UK), pp. 159-202.

Pierson, T.C., Costa, J.E., 1987. A rheologic classification of subaerial sediment-water flows, in: Costa, J.E., Wieczorek, G.F. (Eds.), Debris flows/Avalanches: Process, Recognition, and Mitigation. Geological Society of America Reviews in Engineering Geology 7, pp. 1-12.

Porfido, S., Esposito, E., Alaia, F., Molisso, F., Sacchi, M., 2009. The use of documentary sources for reconstructing flood chronologies on the Amalfi rocky coast (southern Italy), in: Violante, C. (Eds.), Geohazard in Rocky Coastal Areas. Geological Society, Special publication 322, London, pp. 173–187.

Prosser, I., Williams, L., 1998. The effect of wildfire on runoff and erosion in native Eucalyptus forest. Hydrological Processes 12, 251–265.

Regelink, I.C., Stoof, C.R., Rousseva, S., Weng, L., Lair, G.J., Kram, P., Nikolaidis, N.P., Kercheva, M., Banwart, S., Comans, R.N.J., 2015. Linkages between aggregate formation, porosity and soil chemical properties. Geoderma 247-248, 24-37.

Regional Department of Agriculture, 2013. Piano antincedio boschivo 2013. http://www.agricoltura.regione.campania.it/comunicati/pdf/AIB_2013.pdf (accessed 02.10.2016)

Riley, K. L., Bendick, R., Hyde, K.D., Gabet, E.J., 2013. Frequency–magnitude distribution of debris flows compiled from global data, and comparison with post-fire debris flows in the western U.S. Geomorphology 191, 118-128.

Robertson, S., 2011. Direct Estimation of Organic Matter by Loss on Ignition: Methods. http://www.sfu.ca/soils/lab_documents/Estimation_Of_Organic_Matter_By_LOI.pdf (accessed 20.7.15).

Robichaud, P.R., Wagenbrenner, J.W., Lewis, S.A., Ashmun, L.E., Brown, R.E., Wohlgemuth PM. 2013. Post-fire mulching for runoff and erosion mitigation Part II: effectiveness in reducing runoff and sediment yields from small catchments. Catena 105, 93–111.

Robichaud, P.R., Brown, R.E., 2002. Silt fences: an economical technique for measuring hillslope soil erosion. U.S. Department of Agriculture, Forest Service, Rocky Mountain Research Station, Fort Collins, Colorado. Gen. Tech. Rep. RMRS-GTR-94.

Rodríguez, A., Guerra, J.A., Gorrín, S.P., Arbelo, C.D., Mora, J.L., 2002. Aggregates stability and water erosion in andosols of the Canary islands. Land Degradation & Development 13, 515-523.

Rolandi, G., Petrosino, P., McGeehin, J., 1998. The interplinian activity at Somma-Vesuvius in the last 3500 years. Journal of Volcanology and Geothermal Research 82, 19-52.

Rosso, R., Rulli, M.C., Bocciola, D., 2007. Transient catchment hydrology after wildfires in a Mediterranean basin: runoff, sediment and woody debris. Hydrology and Earth System Sciences 11(1), 125-140.

Rulli, M.C., Offeddu, L., Santini, M., 2013. Modeling post-fire water erosion mitigation strategies. Hydrology and Earth System Sciences 17, 2323-2337.

Rulli, M.C., Spada, M., Bozzi, S., Bocchiola, D., Rosso, R., 2006. Rainfall simulations on a fire disturbed Mediterranean area. Journal of Hydrology 327, 323-338.

Santi, P., Cannon, S., DeGraff, J., 2013. Wildfire and Landscape Change, in: Shroder, J. (Editor in Chief), James, L.A., Harden, C.P., Clague, J.J. (Eds.), Treatise on Geomorphology. Academic Press, San Diego, CA, Vol. 13, Geomorphology of Human Disturbances, Climate Change, and Natural Hazards, pp. 262–287.

Santo, A., Di Crescenzo, G., Del Prete, S., Di Iorio, L., 2012. The Ischia island flash flood of November 2009 (Italy): Phenomenon analysis and flood hazard. Physics and Chemistry of the Earth 49, 3–17.

Scott, K.M., 1988. Origins, behavior, and sedimentology of lahars and lahar-runout flows in theToutle-Cowlitz system. U.S. geol. Survey Prof. Paper 1447-A: 1-74.

Shakesby, R.A., 2011. Post-wildfire soil erosion in the Mediterranean: Review and future research directions. Earth-Science Reviews 105, 71-100.

Shakesby, R.A., Doerr, S.H., 2006. Wildfire as a hydrological and geomorphological agent. Earth-Science Reviews 74, 269–307.

Shakesby, R.A., Chafer, C.J., Doerr, S.H., Blake, W.H., Wallbrink, P., Humphreys G.S., Harrington B.A., 2003. Fire severity, water repellency characteristics and hydrogeomorphological changes following the Christmas 2001 Sydney forest fires. Australian Geographer 34, 147–175.

Staley, D.M., Wasklewicz, T.A., Kean, J.W., 2014. Characterizing the primary material sources and dominant erosional processes for post-fire debris-flow initiation in a headwater basin using multi-temporal terrestrial laser scanning data. Geomorphology 214, 324-338.

Stefanidis, P., Sapountzis, M., Stathis, D. 2002. Sheet erosion after fire at the urban forest of Thessaloniki (Northern Greece). Silva Balcanica 2, 65-77.

Summa, V., Tateo, F., Medici, L., Giannossi, M.L., 2007. The role of mineralogy, geochemistry and grain size in badland development in Pisticci (Basilicata, Southern Italy). Earth Surface Processes and Landforms 32, 980-997.

Swanson, F.J., 1981. Fire and geomorphic processes, in: Mooney, H.A., Bonnicksen, T.M., Christiansen, N.L., Lotan, J.E., Reiners, W.A. (Eds.), Fire Regime and Ecosystem Properties. United States Department of Agriculture, Forest Service, General Technical Report WO, 26, United States Government Planning Office, Washington DC, pp. 401–421.

Terribile, F., Basile, A., De Mascellis, R., Iamarino, M., Magliulo, P., Pepe S., Vingiani S., 2007. Landslide processes and Andosols: the case study of the Campania region Italy, in: Arnalds, et al. (Eds.), Soils of Volcanic Regions in Europe. Springer-Verlag, Berlin, pp. 545-563.

Tiranti, D., Moscariello, A., Giudici, I., Rabuffetti, D., Cremonini, R., Campana, V., Bosco, F., Giardino, M., 2006. Post-fire rainfall events influence on debris-flows trigger mechanisms, evolution and sedimentary processes: the Rio Casella case study in the

North-western Italian Alps, in: EGU General Assembly 2006 Geophysical Research Abstracts, Vol. 8, 03479, 2006 SRef-ID: 1607-7962/gra/EGU06-A-03479 © European Geosciences Union 2006.

Tranfaglia, G., Braca, G., 2004. Analisi idrologica e meteorologica dell'evento alluvionale del 24–25 Ottobre 1954: confronto con le serie storiche e valutazione del periodo di ritorno di eventi analoghi, in: Esposito, E., Porfido, S., Violante, C. (Eds.), Il nubifragio dell'Ottobre 1954 a Vietri sul mare. Costa d'Amalfi, Salerno. Pubblicazione G.N.D.C.I. n. 2870, pp. 295–348.

US Environmental Protection Agency (EPA) Method 3051, 1998. Microwave assisted acid digestion of sediments, sludge, soils and oils. January 1998. US EPA Office of Solid Waste. Washington D.C.

US Environmental Protection Agency (EPA) Method 3052, 1996. Microwave assisted acid digestion of siliceous and organically based matrices. December 1996. US EPA Office of Solid Waste. Washington D.C.

Vafeidis, A.T., Drake, N.A., Wainwright, J., 2007. A proposed method for modelling the hydrologic response of catchments to burning with the use of remote sensing and GIS. Catena 70, 396-409.

VanDine, D.F., Rodman, R.F., Jordan, P., Dupas, J., 2005. Kuskonook Creek, an example of a debris flow analysis. Landslides 2, 257-265.

Warkentin, B.P., 1984. Physical properties of forest-nursery soils: relation to seedling growth, in: Duryea ML, Landis TD, editors. Forest nursery manual: production of bareroot seedlings. Boston (MA): Martinus Nijhoff/Dr W Junk Publishers, pp. 53-62.

Wells, W.G., Wohlgemuth P.M., 1987. Sediment traps for measuring on slope surface sediment movement. USDA Forest Service, Berkeley, California. Research Note PSW-393.

Wondzell, S.M., King, J.G., 2003. Postfire erosional processes in the Pacific Northwest and Rocky Mountain regions. Forest Ecology and Management 178, 75–87.

WRB, 2006. World reference base for soil resources 2006. Reports, 103, FAO Press, Rome, Italy.

Web references

Crystallographic and Crystallochemical Database for Minerals and their Structural Analogues. http://database.iem.ac.ru/mincryst/index.php (accessed 1.2.16).

Weather forecast bulletin emitted by the Regional Civil Protection http://bollettinimeteo.regione.campania.it/?m=201209&paged=6 (accessed 5.1.16).

Tables

Parameters	Watershed	Burned area
area (ha)	55	11
perimeter (km)	3.343	1.610
slope min (°)	2	2
slope max (°)	58	54
slope range (°)	55.9	52
slope average (°)	34.9	34.8
alt min (m)	246	246
alt max (m)	891	560
relief ratio	0.45	--
main channel length (m)	1432	--
main channel slope (°)	23	--
main channel slope at outlet (°)	11	--

1 Table 1. Summary of some morphometric parameters related to the Sant'Angelo Creek
2 watershed and to the burned area.

DEPTH (cm)	WDPT (s)							
	MODERATE SOIL BURN SEVERITY			HIGH SOIL BURN SEVERITY				
0	17	3	16	0	0	0	5	3
1	45	5	12	12	> 1900	10	25	18
2	15	18	39	160	> 1900	65	115	95
3	15	22	43	600	> 1900	150	348	110
4	18	38	41	> 1900	1536	800	> 1900	175
5	2	32	28	> 1900	1320	> 1900	> 1900	280
6	2	12	11	> 1900	10	> 1900	> 1900	1520
7	30	6	8	0	5	1200	> 1900	1568
8	10	4	5	0	2	22	10	1762
9	2	1	0	0	1	0	0	973
10	0	1	0	0	0	3	0	24

Table 2. WDPT test results performed in the areas burned with moderate and high soil burn severity.

RAIN GAUGE	RAINSTORM TIME INTERVAL (hours)	TOTAL STORM RAINFALL (mm)	I_{10} (mm/h)	I_{30} (mm/h)	DISTANCE FROM THE STUDY WATERSHED (km)
CETRONICO	04:50 - 6:30	23.8	37.2	30.8	4
BRACIGLIANO	04:50 - 6:20	22.2	37.2	25.2	4.4
PIANI DI PRATO	04:40 - 5:50	13.2	19.2	15.6	2.8

1

2 Table 3. Rainfall data collected by the Civil Protection rain gauges used in this study.

SAMPLE	TEXTURE	COLOR	% COMPONENTS (Phi-1÷1)			GRAIN SIZE PROPERTIES				G_s (g cm^{-3})	SOM (%)	W (%)	W_{AV} (%)
			Vege-table	*Vol-canic*	*Carbo-nate*	Mz (phi)	s (phi)	Sk (phi)	Kg (phi)				
B1	Gravelly muddy sand	Dark brown 10 YR 3/3	0 - 15	85 - 100	0	1.72	3.33	0.47	2.68	2.1	9.9	12	11.5
B2	Gravelly muddy sand	Brown 2.5 Y 3/2	< 5 - 10	90 - 95	0	2.42	3.32	0.29	2.11	2.3	8.4	11	
NB1	Gravelly muddy sand	Dark olive brown 2.5 Y 3/3	0 - 10	90 - 100	0	1.76	3.39	0.45	2.48	2.2	10.3	13	
NB2	Gravelly muddy sand	Dark grayish brown 2.5 Y 4/2	0 - 30	70 - 95	0-5	2.22	3.42	0.27	2.02	2.2	9.6	10	
D1	Muddy sandy gravel	Brown 2.5 Y 3/2	0	95	0-5	0.44	2.61	0.92	5.75	2.4	2.5	41	42
D2	Gravelly mud	Brown 2.5 Y 3/2	30 - 70	30 - 70	0	5.58	1.79	-0.56	4.92	1.9	27	43	

Table 4. Summary of the results obtained by laboratory analysis (Mz = mean particle size; s = sorting; Sk = skewness; Kg = Kurtosis; Gs = specific gravity; SOM = soil organic matter; W = water content; W_{AV} = average water content). Sample textures (Folk, 1974) are also indicated.

Element (ppm)	B1	NB1	B2	NB2
Aluminum	42660	42670	41740	44520
Barium	995	840	777	827
Calcium	18670	18550	18160	20160
Iron	19880	17540	18510	19770
Magnesium	7363	6659	7530	6928
Manganese	575.9	467.	526	546
Potassium	34770	31950	28770	27950
Sodium	9325	7574	6241	7346
Strontium	436	380	358	366
Titanium	1848	1448	1582	1677

Table 5. Amount of the inorganic elements measured in the burned and unburned soil samples.

Sample	Moisture (%)	Volatiles (%)	Ashes (%)	Fixed Carbon
B1	2.3	6.7	91.0	-
B2	2.6	8.6	88.4	0.44
NB1	2.2	6.6	91.2	-
NB2	3.1	9.0	87.9	1.4

Table 6. Proximate Analysis results

Post-fire erosion response in a watershed mantled by volcaniclastic deposits, Sarno Mountains, Southern Italy

Giuseppe Esposito[a], Fabio Matano[a], Flavia Molisso[a], Giovanna Ruoppolo[b], Almerinda Di Benedetto[c], Marco Sacchi[a]

[a] Consiglio Nazionale delle Ricerche - Istituto per l'Ambiente Marino Costiero (CNR-IAMC), Calata Porta di Massa - Porto di Napoli, 80133 Napoli, Italy

[b] Consiglio Nazionale delle Ricerche - Istituto di Ricerche sulla Combustione (CNR-IRC), Piazzale V. Tecchio 80, 80125 Napoli, Italy

[c] Dipartimento di Ingegneria Chimica, dei Materiali e della Produzione Industriale, Università di Napoli Federico II, Piazzale V. Tecchio 80, 80125 Napoli, Italy

Corresponding author: Giuseppe Esposito, CNR-IAMC, Calata Porta di Massa - Porto di Napoli, 80133 Napoli, e-mail: giuseppe.esposito@iamc.cnr.it, tel.: +39 0815423834

Abstract

In this study we document a post-fire erosion response to a short-lived, intense rainstorm occurred on 6 September, 2012 in the Sant'Angelo creek watershed, Sarno Mountains, Southern Italy. The rainstorm occurred one month after a wildfire that burned about 11 ha of the steep watershed (55 ha), almost entirely mantled by volcaniclastic deposits. The research was based on fieldwork and laboratory analysis addressed to the understanding of the geomorphic effects of the wildfire and their impact on erosional and depositional processes triggered by subsequent rainstorms. Field evidence indicates that a series of overland flows caused significant runoff and sediment yields along the hillslope and accumulation of hyperconcentrated flow deposits in a concrete channel occluded by a sealed culvert at the outlet of the watershed. The results of geomorphological and sedimentological analysis suggest that the occurrence of volcaniclastic covers mantling the slopes likely favored accelerated soil erosion, especially where vegetation and litter had been removed by the fire. Chemical analysis on sediment samples, revealed the occurrence of iron oxides that enhanced soil water repellency conditions over wide areas of the burned watershed compared to the unburned areas.

Quantitative analysis of sediment budgets showed that the rainfall-induced erosion response at Sant'Angelo creek watershed resulted in a soil loss of 19.8 - 33.1 tons ha^{-1} over burned areas. Post-fire erosion response following severe rainstorms needs to be considered in the spectrum of natural hazards associated with the geomorphological evolution of mountainous landscapes mantled by volcaniclastic deposits.

Keywords: wildfire; rainstorm; post-fire erosion response; soil loss; Sarno Mountains.

1 Introduction

During the last decade, the role of wildfires as geomorphic agent has been widely recognized by the scientific community (e.g. Moody et al., 2013). Direct effects of wildfires on soil and vegetation (e.g. Certini, 2005; Shakesby and Doerr, 2006; Jordàn et al., 2013) may enhance erosion through sheetwash and rilling processes, often resulting in large mass movements (Swanson, 1981; Cannon et al., 1998; Wondzell and King, 2003; Nyman et al., 2011; Moody et al., 2013; Riley et al., 2013; Santi et al., 2013). Post-fire erosion responses may have a variety of impacts on landscapes. For instance, they can dominate the long-term sediment yield in a given area, until the geomorphic system returns to the typical conditions of unburnt terrain (Swanson, 1981; Prosser and Williams, 1998; Shakesby, 2011). Moreover, they represent a severe risk for human life, where houses and other infrastructures occur (Cannon and DeGraff, 2009; Nyman et al., 2011). Post-fire catastrophic floods and deadly debris or sediment-laden flows have been reported from several areas of Canada, western United States and southeastern Australia (e.g. Moody et al., 2013; Kean et al., 2011; VanDine et al., 2005; Nyman, 2013). In the Mediterranean region, prevailingly moderate fire-related erosional events have been documented. However, as pointed out by Parise and Cannon (2008), most of research works in this area have dealt with experimental plots (e.g. Rosso et al., 2007) rather than analysis of post-wildfire landslides and erosional events. Case studies reported for Mediterranean region have mostly focused on Spain and Portugal (e.g. Lorente et al., 2002, 2003; Beguería, 2006; García-Ruiz et al., 2010, 2013; Lourenço et al., 2012) and fewer on the central countries, like in Italy and Greece (e.g. De vita et al., 1994; Tiranti et al., 2006; Calcaterra et al., 2007; Stefanidis et al., 2002; Blake et al., 2010).

The majority of the Mediterranean study areas are characterized by thin, stony soils, where surface erosion after wildfires is supply-limited with erosion rates ranging between

0.016 and 13.1 t ha^{-1} y^{-1} (Shakesby, 2011). A notable exception is represented by the volcanic areas of southern Italy, where local abundance of fine-grained, loose volcaniclastic material lying on steep volcanic and/or calcareous slopes may be observed (De Vita et al., 2006; Matano et al., 2016). Such material is often associated with andosols (WRB, 2006) characterized by relatively low cohesion under dry conditions (Maeda et al., 1977; Warkentin, 1984) and high erodibility when slope-stabilizing vegetation is absent (Rodriguez et al., 2002). The occurrence of wildfires in volcaniclastic settings is often reported, in fact, as a condition that enhances the probability of massive sediment-laden flows, as observed by Meyer and Wells (1997) in the Yellowstone National Park (U.S.A) and by Neris et al. (2016) in the Canary Islands (Spain). Nevertheless, according to Neris et al. (2016), hydrological and erosional response of this terrain type in the post-fire period has received little attention by the scientific community.

A distinctive feature of several regions of the central Mediterranean area is the local abundance of sediment-supplying soils occurring in steep slopes characterized by a plenty of easily flammable shrubs and forests. Such increase in the natural fuel load can be enhanced by inappropriate land use and/or land abandonment and afforestation with highly flammable species (Shakesby, 2011). Due to the combination of these factors with a likely increase in the frequency of extreme climatic events through time (Arca et al., 2010; Moriondo et al., 2006), future wildfire activity is expected to increase in the overall Mediterranean area.

In this study we document a post-fire erosion response to a short-duration, high-intensity rainstorm that occurred in the Sant'Angelo creek watershed, Sarno Mountain Range, southern Italy (Fig. 1). This area, characterized by a Mesozoic carbonate bedrock covered by pyroclastic deposits and andosols, was partially burned on 4 August, 2012 (Esposito et al., 2013) and hit by a first rainstorm on 6 September, 2012.

The aims of this study are: (i) to improve knowledge about fire effects and related soil erosion processes in steep slopes covered by volcanic soils; (ii) to highlight that high amount of soil loss can occur in such contexts; (iii) to give a valid contribution towards the documentation of post-fire erosion responses occurring in the central Mediterranean area.

The research work was based on a multidisciplinary approach integrating fieldwork with chemical, mineralogical and grain size analysis conducted on soil samples collected in the study area. Similar approach was adopted in other erosional contexts of southern Italy (e.g. Summa et al., 2007; De Santis et al., 2010), demonstrating to be very suitable to investigate the effects and causes of erosion. Laboratory and field data were also used to quantify soil loss at the watershed scale.

2 The Sant'Angelo Creek watershed

2.1 Geological background

The Sant'Angelo Creek watershed is located in the Sarno Mountain Range, along the southern slope of Mt. Torrenone, about 3 km east of the town of Sarno (Fig. 1). The ridge is mainly formed by bedded Mesozoic carbonates (Di Nocera et al., 2011) and since the Late Quaternary it has been repeatedly mantled by pyroclastic airfall deposits, as a result of explosive activity of the Somma-Vesuvius (Rolandi et al., 1998) and Campi Flegrei (Orsi et al., 1996) volcanic districts (Fig. 1).

At the Sant'Angelo Creek watershed, the thickness of the volcaniclastic cover may vary significantly in different areas (Fig. 2), and it reaches a maximum of 5 m (De Vita et al., 2006; Autorità di Bacino del Sarno, 2011). However, slope-mantling deposits may be locally much thinner due to previous erosion and/or recent landslides. Figure 2 reports the areal distribution of the varying thickness of volcaniclastic deposits that have been grouped into three classes (0.1-0.5 m; 0.5-2.0 m; 2.0-5.0 m), whereas carbonate scarps

are referred to as exposed bedrock. The map indicates that in the burned area, the thickness of the pyroclastic cover mostly ranges from 0,5 m to 2,0 m. These volcaniclastic deposits are typically interbedded with a series of soil horizons classified as andosols (WRB, 2006), and characterized by a high content of glass and amorphous colloidal materials, including allophane and imogolite, and andic features ranging from high (Alo+0,5Feo>2%) to moderate (Alo+0,5Feo:1-2%) (Terribile et al., 2007).

2.2 Geomorphological setting

The morphology of the Sarno Mts. is marked by several tectonic lineaments (i.e. fault slopes) and carbonate scarps, along with gullies and karstic features with high gradients. Gullies are incised up to 30 m, and extend downslope from the ridge crest. Slope profiles are marked by a series of narrow scarps that may be followed laterally up to a few hundred meters. The scarps display heights ranging from 1-2 m to 10-15 m and typically correspond to erosion profiles of thick carbonate beds. Morphometric parameters of the Sant'Angelo creek watershed are summarized in Table 1, and a slope map of the watershed is showed in Fig. 2. Hillslopes are characterized by an average slope angle of about 35°. A marked decrease in the slope angles from 23° to 11° occurs along the channel slope at the outlet of the watershed.

The recent geomorphological evolution of the mountain range has been characterized by areal erosion along hillslopes with poor or absent vegetation, as well as by linear erosion along major valley axes. The most common instability processes in the study area are represented by rock falls affecting fractured carbonate scarps, and shallow landslides often involving the volcaniclastic covers. The Sarno Mountain Range area was also hit by a series of landslides evolving in downstream debris flows that occurred on 4-5 may 1998, after a period of prolonged rainfall (120 mm of cumulated rainfall in 48 hours). The event caused 137 deaths in the town of Sarno (Cascini et al., 2008), and involved the

volcaniclastic deposits and soils covering the carbonate slopes (Guadagno et al., 2005; De Vita et al., 2013). The slope instability, in this case, was mostly due to deterioration of mechanical properties of the volcaniclastic covers, as a consequence of the concentrated rainfalls and of the specific hydrological and geotechnical conditions (Cascini et al, 2003, 2013), which is substantially different from the post-fire erosional phenomena discussed in this work.

2.3 Meteo-climatic factors

The Sarno region is characterized by a typical Mediterranean climatic regime with hot, dry summers and moderately cool, rainy winters (Ducci and Tranfaglia, 2008). The annual average precipitation of this inner sector of the Apennines is in the order of 1000 mm/year at lower altitudes and 1400-1500 mm/year over summit areas.

In this part of the Mediterranean region, the major rainstorms following the peak summer period are caused by the Tropical-Like Cyclones (TLC), most of which occur between August and November (Tranfaglia and Braca, 2004; De Luca et al., 2010). Rainfalls from TLC are typically very intense and generally concentrated over small areas. Such meteorological systems, together with frontal storms and isolated convective cells, are able to trigger significant landslide phenomena, flash floods and debris flows (De Vita et al., 1994; Esposito et al., 2004; Esposito et al., 2015; Calcaterra et al., 2007; Porfido et al., 2009; Ciervo et al., 2012; Santo et al., 2012).

2.4 Fire regime

As in other Mediterranean countries, the occurrence of wildfires in Italy is concentrated during the hot and dry summer months, between July and September. The Italian territory extends over an area of 30.134 x 10^6 ha and, according to the State Forestry Corps (JRC, 2015), 8700 fires per year averaged in the period 1970-2015, burning about 100000 ha/yr.

The Sant'Angelo creek fire is one of the 8252 fires that burned 130814 ha through the country in 2012. According to the State Forestry Corps, none of these events was related to natural causes, thus pointing at human responsibility in the ignition of many fires (JRC, 2013). Campania (Fig. 1) is one of the Italian regions most affected by fires. According to the Regional Department of Agriculture (2013), during 1991-2013, 60612 fires (average = 2635) burned a total surface of 161680 ha (average = 7030 ha). A remarkable number of these events affected the woodlands of the Sarno Mountains. In this area, in fact, 135 documented fires occurred in the period 2005-2015. The total burnt surface was 1118 ha, with an average fire size of 8 ha that is little less than the estimated average of 12 ha for Italy (JRC, 2015). In 2012, in addition to the Sant'Angelo creek fire, other 28 events hit the Sarno Mountain Range, causing a total burnt surface of about 220 ha.

3 Materials and methods

This research was based on integration of: a) geological and geomorphological data and soil burn severity assessment carried out at Sant'Angelo creek watershed during fieldwork; b) rainfall time series relevant to the analysis of the 6 September, 2012 meteorological event and c) sedimentological and chemical analysis of soil and sediment samples collected from the study area. Analysis of data included interpretation of geomorphic processes that developed along Sant'Angelo creek watershed and computation of erosion/deposition volumes of sediments involved in the post-fire response.

3.1 Analysis of geological and morphological data

Analysis of geological and morphological data of Sant'Angelo creek watershed was conducted through spatial analyst tools of ArcGIS 10.3^{TM}. As input data, we used a digital tridimensional model (DTM) of the watershed with a cell size of 5 m, and soil thickness data (Autorità di Bacino del Sarno, 2011). Data analysis allowed for extrapolation of

morphometric properties of the study watershed and the construction of a thickness map of the pyroclastic covers. Results of this analysis are summarized in Table 1 and Figure 2.

3.2 Rainfall data

We analyzed data collected from three rain gauges located near the study area (Fig. 1). The most representative among these is the “Cetronico” rain gauge, located at a distance of 4.5 km to the east, along the same drainage divide with respect to the study area. All rainfall time series have been recorded at a sampling rate of 10 minutes. Relevant parameters derived from data acquired by the “Cetronico” rain gauge during the 6 September rainfall include: a) daily cumulative rainfall depth and 10-minute peak intensity (I_{10}); b) 30-minute rainfall intensity (I_{30}); c) total storm rainfall and duration; d) cumulative rainfall intensity and e) depth profiles. For the two other rain gauges only the total storm rainfall, duration, I_{10} and I_{30} are reported for comparisons.

3.3 Fieldwork data

The field survey started the day after the erosion response and involved both the study watershed and neighboring areas in order to verify the areal extension of erosional processes across the boundary between burned and unburned areas.

Qualitative metrics suggested by Parsons et al. (2010) were used to assess soil burn severity, which require evaluation of vegetation condition, soil water repellency, surface color and root condition. The persistency of soil water repellency was detected by in situ Water Drop Penetration Time (WDPT) tests, following the method of DeBano (1981). In all sites, five pits were carried out and, in each of them, WDPT tests were performed from the soil surface until a depth of 10 cm, with a step of 1 cm. The median time between the five replications was used as the WDPT for each depth. The results of soil burn severity

assessment were summarized into two classes and then mapped in a soil burn severity map.

3.4 Sedimentological, chemical and mineralogical analyses

Laboratory analysis was conducted on samples collected from the areas characterized by high soil burn severity (B1 and B2) as well as from the outside of the burned area (NB1 and NB2) (Fig. 3). All samples were representative of the bulk of the uppermost soil horizon from the surface down to a depth of ca.10 cm.

Soil samples were processed for grain size, chemical and mineralogical analysis (e.g. Summa et al., 2007). The results of laboratory analyses on these samples have provided relevant information to identify physical or chemical alteration of soils induced by fire that likely controlled the triggering mechanisms of erosion processes.

Two additional sediment samples (D1 and D2) were collected respectively from the tail and the front of a deposit observed after the 6 September 2012 rainstorm and trapped within the concrete channel at the outlet of the watershed (Fig. 3). For all samples ca. 300 g of material was collected.

Both sediment and soil samples were processed for grain size analysis, estimation of organic matter and water content, and specific gravity. The nature and percentage occurrence of constituents was determined using a Leica Zoom 2000 stereo microscope. The distribution of grain size fraction > 0.0125 mm was determined by sieve analysis, whereas the fraction < 0.0125 mm was analyzed by laser diffractometry (Sympatec). Grain size statistical parameters including mean particle size, sorting, skewness and kurtosis have been calculated following the classic graphical method of Folk and Ward (1957).

The organic matter content of samples (SOM) was estimated following the LOI (Loss on Ignition) procedure suggested by Robertson (2011). The water content was evaluated by

the gravimetric method. Specific gravity was calculated following the ASTM D-854 (2010) and the soil color was determined using a Munsell Soil Color Charts (1994).

Soil samples were also processed for the determination of major physical properties and chemical composition. An inorganic elemental analysis was conducted by inductively coupled plasma mass spectrometry (ICP-MS), using an Agilent 7500CE instrument after dissolving the fuel samples by means of microwave-assisted acid digestion, according to US-EPA 3051 and 3052. The soil modification after the fire was evaluated by measuring moisture, volatile, fixed carbon and ash content using a TGA 701 LECO thermo-gravimetric analyzer, according to the ASTM D-5142 standards.

Soil samples were processed for X-ray diffraction (XRD) using a PW 1100 Philips diffractometer in order to analyze the crystalline species. The obtained spectra were interpreted using the WWW-MINCRYST: Crystallographic and Crystallochemical Database for Minerals and their Structural Analogues. The morphology of materials was investigated with a FEI Inspect S SEM microscope.

3.5 Sediment erosion and deposition budgets

The post-fire erosion response that occurred on September 2012 at the Sant'Angelo creek watershed produced a massive deposit at the outlet of the watershed that was trapped in an artificial channel closed by a blocked culvert. In this case, the sealed channel acted as a watershed-scale sediment trap (Wells and Wohlgemuth, 1987; Robichaud and Brown, 2002; Morris et al., 2011) allowing for a computation of volume and weight of trapped sediments and a reliable estimate of the soil loss per unit area along the burned hillslope.
In order to estimate the total volume and weight of the soil mobilized by erosional processes along the hillslope and compare it with the weight of the deposits that have been found both within the artificial channel and along the slopes, two metrics were

collected during the fieldwork: 1) thickness of eroded soil around the tree bases and 2) thickness of eroded soil by rills or rill depth (see section 4.3.1). These data were interpolated in ArcGis 10.3^{TM} software, in order to identify and map the areas characterized by the mobilized amounts of soil and their volumes. The weight corresponding to all measured volumes were calculated by using specific gravity derived from the study soil samples.

4 Data analysis and results

4.1 Soil burn severity

The fieldwork conducted in this study was specifically addressed to verify the occurrence of fire effects on vegetation and soil properties and eventually evaluate their spatial variability.

During the survey, we have observed that in some areas the crowns of oak trees were not completely leafless, the scorched leaves on trees had a light brown color and branches were only partially scorched. The surficial color was brown and a number of smaller roots near surface were slightly charred. Moreover, WDPT data, classified according with Bisdom et al. (1993), showed a slight water repellency characterized by infiltration times of 2-45 seconds (Table 2).

In other areas, there was evidence that some oak trees were bent by the winds during the fire and no leaves on their fully charred branches were detected. A black charred ground surface was common and both small and larger roots were entirely charred near the surface, where a ca. 10 cm thick layer of litter, duff and bushes was destroyed by the flames. In these areas, WDPT tests revealed severe water repellency reflected by infiltration times also higher than half an hour (Table 2). Furthermore, rock fragments spalled during the fire were also found at the base of some charred carbonate outcrops.

Following the suggestion of Parsons et al. (2010), these effects were used to discriminate among different soil burn severity classes. The soil burn severity map represented in Fig. 3 illustrates the extent and the various degrees of severity burned areas. Particularly, the map shows that the area characterized by high soil burn severity represents 65% of the 11 ha total burned surface, whereas the area corresponding to moderate soil burn severity, represents the 35% of the surface. The figure also indicates the location of soil and sediment sampling sites, WDPT test sites, and the path of the debris flow that struck the area of Sarno in 1998.

4.2 Rainfall properties

The post-fire response discussed in this work was triggered by a rainstorm generated within the tail of a low-pressure vortex formed above the Tyrrhenian Sea, off the Italian west coast (Weather forecast bulletin emitted by the Regional Civil Protection on 5 September, 2012). The storm had a radius of ca. 5 km and it was recorded by all the three rain gauges available for the study area (Table 3).

Particularly, the daily rainfall data of Cetronico gauge indicate that the precipitation over Sant'Angelo Creek watershed on 6 September, 2012 was characterized by both the highest 10-minute rainfall intensities and rain depths after the fire (Fig. 4). The rain gauge, recorded a total storm rainfall of 23.8 mm between 04:50 and 06:30 of that day. Within this time interval, 15.4 mm of rainfall occurred in the first 30 minutes (between 4:50 and 5:20), with a 30-minute peak rainfall intensity (I_{30}) of 30.8 mm/h (Fig. 5). The 10-minute peak storm intensity (I_{10}) of 37.2 mm/h was reached between 5:10 and 5:20.

The inset of Fig. 5 shows that the rainfall intensity profile (black line) of the storm is characterized by a rapid rise with a peak followed by a relatively slow decline. The cumulative rainfall depth profile (gray line) also shows an initial rapid rise followed by a

slower increase, thus confirming the character of short-duration, high-intensity convective of the storm.

4.3 Field indicators of post-fire geomorphic processes

4.3.1 Indicators of erosional processes

Several field indicators of erosional and depositional processes were identified during the field survey. Evidence of recent instability were not observed outside the burned parts of the watershed, where the vegetation cover is composed of 10 cm-thick litter, oak trees and the typical Mediterranean scrub (Fig. 6). Moreover, we did not observe any evidence of flow processes or deposits at the outlet of the nearby unburned watersheds during the survey.

Evidences of recent erosional processes detected on the slopes are summarized below.

1) Patches of crusted soil were identified locally. They are characterized by lighter color and higher compaction with respect to the adjacent surrounding areas. WDPT tests performed on the surface consistently revealed a lack of infiltration capacity for an average thickness of 3 cm. The extension of individual patches is in the order of a few square decimeters.
2) Along the main runoff path, some aligned trees characterized by light annular bands at their base were detected (Fig. 7A). These bands correspond to parts of the bark that were covered by soil during wildfire, and became visible after post-fire erosion processes acted along the burned hillslope. The bands displayed a height of 2 - 8 cm and were often associated with bared roots (Fig. 7B).
3) A dozen of rill networks were also found in the burned area. Specifically, they were located where the fire burned with high soil burn severity, along the lower sector of slopes characterized by gradients of ca. 35° (Fig. 8). All networks appeared to be

interrupted at slope breaks. Rills had a maximum length of ca. 10 m and a depth in the order of 10 - 20 cm. Individual rill scours had a width of 10 - 20 cm and no levees were detected along their margins.

Field data, including the height of the light bands at the base of the trees, and rill depth along burned slopes, suggest that the total volume of soil eroded along the burned hillslope was ca. 186 m^3. By considering a specific gravity of 2.2 g/cm^3 and a water content of 11.5 % for burned soils (Table 4), the resulting dry weight of the eroded material is ca. 364 tons.

4.3.2 Indicators of depositional processes

Several indicators of depositional processes were found both at the watershed outlet and along the burned slopes. The deposit found in the artificial channel at the outlet of the watershed (Fig. 9) is represented by mineral soil particles, ash, and charred plant remains. The concrete structure was built after the Sarno 1998 catastrophic landslide event, in order to funnel possible future debris flows into large storage basins downstream, and remained empty until the 6 September, 2012 rainstorm (see Google Earth historical images captured on 6/1/2010 and 7/14/2012 - 40°48'44.83"N, 14°39'40.28"E).

Field investigation showed that sediment and debris accumulation along the artificial channel was partly induced by the lack of maintenance of the culvert, with consequent obstruction of the hydraulic section, that caused a damming effect at the base of the channel. Traces of mud (Fig. 9) and splash marks were detected on the concrete banks.

The volume of flow deposit accumulated into the channel was estimated in ca. 175 m^3. Considering a specific gravity of 2.15 g/cm^3 and an average water content of 42 % (Table 4), the resulting dry weight of the deposit is ca. 218 tons.

Significant accumulation of sediments was found locally over the slopes, either behind the base of larger living trunks (Fig. 10), or trapped by the damming caused by charred

branches and trunks intercepting runoff. Furthermore, patches of liquefied soil were found over carbonate scarps, locally filling-up the rough morphology. At least twenty areas of sediment and soil accumulation have been detected along the slope, with a cumulative volume of material of ca. 55 m^3, corresponding to an estimated total dry weight of ca. 88 tons of deposits.

4.4 Sedimentological characterization

Sedimentological analysis showed that both burned (B1, B2) and unburned (NB1, NB2) soil samples can be classified as gravelly muddy sand (Fig. 11) according to the classification system proposed by Folk (1974). This is also reflected by the similarity of grain size statistical parameters, soil organic matter and specific gravity reported in Table 4. Microscopic analysis showed that all samples had a relatively high volcaniclastic fraction content (70-100 %) and a low content of plant remains (0-30 %).

The sediment samples collected into the channel correspond to muddy sandy gravel (D1) and gravelly mud (D2) (Fig. 11). D1 is very poorly sorted (σ_G = 2.61) whereas D2 is poorly sorted (σ_G = 1.79). In terms of composition, sample D1 mostly consist of charred coarse-grained pyroclastic deposits with rare limestone rock fragments, whereas D2 was represented by charred fine-grained volcaniclastics and plant remains (i.e. rootlets, leafs, charcoal and seed fragments). No unburned material was detected into the samples.

Both organic matter content and specific gravity showed significantly different values in the two samples (Table 4). The average water content was 42% whereas in the case of soil samples it was 11.5 %.

A comparison of grain size distribution of samples D1 and D2 with the facies distribution of a post-fire fan deposits (Meyer and Wells, 1997) is showed in Fig. 11. The curves of samples D1 and D2 fall within the hyperconcentrated flow and streamflow fields (Pierson and Costa, 1987), respectively. This evidence is consistent with a significant difference of

sorting ($\sigma_{G\text{-}D1}$ = 2.61 - $\sigma_{G\text{-}D2}$ = 1.79) and with the traces of mud and splash marks detected on the concrete banks (Fig. 9). It also suggests the occurrence of low or no-internal strength turbulent flows characterized by high velocity.

4.5 Chemical/physical and mineralogical characterization

The results of the chemical/physical characterization of soil samples are summarized in Fig. 12 and Table 5 that shows the results of ICP analysis in terms of the concentration of major elements within the samples. The most abundant element is Aluminum (Si is not detected by ICP) followed by K, Ca, Fe, Mg and Na.

It is worth noting that the ICP analysis displays no significant difference between the concentration of the main species of the burned (B) and unburned (NB) soil samples. This suggest that the phenomena occurring during the fire did not alter the inorganic material content. Consequently, only a rearrangement of the inorganic element can be hypothesized. Such results are in agreement with the results of SOM analysis and are also confirmed by the proximate analysis of all the samples given in Table 6, which shows that the content in volatiles is not affected by the exposition to the fire.

The results of the X-ray diffraction (XRD) analysis are shown in Fig. 13. The analysis was performed two times (Batch I, Batch II) for each soil sample in order to assess also the homogeneity of the material. All the XRD spectra show signals (in the range 20-30 of 2σ angle) related to silicate species and more specifically to phyllosilicates and tectosilicates.

In the burned sample, XRD signals at higher angle associated to the occurrence of iron oxides like hematite (Fe_2O_3), magnetite (Fe_3O_4) and wustite (FeO) are present.

The important role of both amorphous and crystalline Fe in stabilizing natural soil aggregates has been proved by many authors. In particular, Jozefaciuk and Czachor (2014) report that an increasing content of Fe causes a decrease in the water stability of small (ca. 1 mm) and large (ca. 1 cm) aggregates.

The morphology of materials was investigated with a FEI Inspect S SEM microscope. The image of the different samples under different magnitude are reported in Fig. 14.

The SEM analysis performed on the NB1 and NB2 samples shows a layered structure composed of phyllosilicates and tectosilicates. The particles show a poor sphericity and roundness and a large size distribution. A comparison of the SEM images of burned and unburned samples suggests that the morphology and the degree of sphericity and roundness are unaffected by the fire.

5 Discussion

5.1 Post-fire geomorphic processes

Morphometric properties showed in Table 1 highlight the occurrence of steep slopes and moderate channel gradients in the Sant'Angelo creek watershed. As widely reported in the literature, steep morphologies may enhance fire intensity and spreading, and increase the potential for surface erosion and mass movements. Indeed the steep topographic conditions of the study area (average slope angle = 35°) may have exerted a significant control on both the soil burn severity and erosional processes.

The results of the fieldwork indicate that the Sant'Angelo creek fire burned 65% of the 11-ha affected area with high severity and 35% with moderate severity. The wildfire caused partial consumption of the tree canopy, shrubs, soil-mantling litter and duff, as well as modification of soil properties (i.e. water repellency). These effects may have been controlled not only by the steep topography but also by high availability of fuel (Fig. 6) and local weather conditions. For instance, a number of bent oak trees found in the burned area suggest, that strong winds occurred during the fire propagation.

Water repellency was investigated in the field through WDPT tests, and showed persistency ranging from slight to severe. The results of mineralogical analysis suggest

that iron oxides, that occur in burned soil samples but are not present in the unburned soil samples, could have enhanced this behavior. Particularly, the occurrence of iron oxides indicates that the upper soil horizon underwent relatively high temperature (250 C) coupled with high oxygen and water content. It has been in fact demonstrated that in highly oxygenated conditions, with high partial pressure, the formation of iron oxides is significantly high (Bertrand et al, 2010).

New aggregates formed by clay, silt and sand particles bound by Fe oxides (Regelink et al., 2015) may lead to a decrease in the soil porosity, which in turn produces a decrease in the soil permeability. According with Gargiulo et al. (2013), iron oxides may cause a 50% reduction of porosity in soils characterized by significant sandy content and low shrinking-swelling capacity. Considering the results of chemical analysis, coupled with mineralogical and textural properties of the analyzed volcanic soils, we infer that a similar mechanism of increased water repellency conditions may have occurred during the Sant'Angelo creek fire. It cannot be excluded that micro-aggregates had formed as hydrophobic compounds generated in the plants litter and migrated downward in the soil along with water vapor and oxygen (DeBano, 2000). Comparison of SEM images with grain size and composition does not indicate any significant structural difference between burned and unburned samples. This would exclude other causes controlling the water repellency conditions.

The rainstorm that occurred in the study area about one month after the fire was characterized by 30-minute peak rainfall intensity (I_{30}) of 30.8 mm/h, triggering a high-magnitude erosion response. A series of indicators recognized during the field survey allowed us to identify the post-fire geomorphic processes triggered by the rainstorm.

Several indicators highlight the occurrence of sheetwash erosion (Shakesby and Doerr, 2006) along the burned hillslope. Clear evidences are the light bands found at the base of some trees (Fig. 7A), indicating the occurrence of overland flows which removed the loose,

friable, and burned mineral soil around the base of the trunks, with a progressive entrainment of material downslope. Suspended sediments transported by overland flows also included soil particles detached during the raindrops impact. As stated by McGuire et al. (2016), steep burned areas characterized by sandy soils may be particularly susceptible to the raindrop-driven detachment process, making the soil surface more erodible and prone to flow-driven transport. Additional evidence of rainsplash detachment is represented by local patches of soil crusts found on the burned slope (Farres, 1987; Le Bissonnais et al.,1989; Mataix-Solera et al., 2011).

The local transition from diffusive erosion dominated by sheetwash to concentrated erosion is testified by rill networks (Fig. 8). The occurrence of rills suggests that, localized Hortonian infiltration-excess may have been a major hillslope-runoff-generating process (e.g. DeBano, 2000). However, it cannot excluded that this process may have included transition and/or switching between infiltration-excess and saturation-excess conditions.
It was not surprising to find rill networks in the burned area, given the high slope gradients (Table 1) and soil burn severity conditions (Fig. 3). In fact, where volcaniclastic deposits occur (e.g. Las Conchas wildfire, Pellettier and Orem, 2014), rilling can be the most common form of hillslope erosion observed in areas characterized by moderate and high soil burn severity.

As detected during field survey, a part of the upper soil horizon including mineral soil particles, ash, charcoal, branches and leaves transported by overland flows was redistributed along the hillslope because of micro-topographic conditions. However, the massive deposit found into the artificial channel at the outlet of watershed (Fig. 9) suggests that about 60% of the mobilized sediments (i.e. 218 of 364 tons) traveled into the main drainage axis of the Sant'Angelo Creek watershed down to the concrete channel, as a gravity flow.

According to what has been observed by Keane et al. (2011) in southern California, we infer that the Sant'Angelo Creek flows possibly initiated shortly after the beginning of the rainfall event, when the estimated 30-minute rainfall intensity (I_{30}) exceeded the threshold value of 20 mm/h for 30 minutes proposed by Cannon et al. (2003 a, b). Decreasing intensity through time (Fig. 5) could have controlled the sediment-water mixture concentration (e.g. Keane et al. 2013). We infer that such variation may have implied transition from hyperconcentrated flow to streamflow (Pierson and Costa, 1987) corresponding to a decrease in the sediment transport capacity towards the final stage of the flow response. The overall grain size diversity between samples D1 and D2 (Fig. 11) may indicate such a tendency. Particularly, we suggest that hyperconcentrated flow deposits may be regarded as the result of massive deposition during the main flow event, whereas streamflow deposits may represent the product of the downstream deposition of flow tail, characterized by abundant fine-grained fraction (sample D2) and plant debris washed away from coarse material deposited upstream (sample D1). The occurrence of similar facies association has been already reported in the literature for post-fire responses in other regions (Meyer and Wells 1997; Cannon et al., 1998; Kean et al., 2011), sometimes with specific reference to lahars in volcaniclastic settings (Scott, 1988; Pierson, 2005). According to Meyer and Wells (1997), burned slopes are broadly analogous to slopes mantled by loose volcaniclastic materials in terms of runoff potential and availability of fine sediment. In this study, due to the coupling of both factors (volcaniclastic materials and burned slope), we suggest that the post-fire flow processes here described could be regarded as of lahar-type.

The results discussed in this section highlight the importance of collecting post-fire field observations, especially in the central Mediterranean area where most of the available studies are based on simulated rainfall and/or experimental plots addressed to the modeling of post-fire erosion responses (e.g. Rulli et al., 2013, 2006; Vafeidis et al., 2007).

Field data are indeed essential to understand mechanisms controlling the initiation and propagation of mass movements (e.g. Cannon et al., 2001; Nyman et al., 2011), and provide useful information to calibrate both models for predicting runoff-generated erosion (Nyman et al., 2015; Kean et al., 2013) and compile catalogues related to post-fire events (Gartner et al., 2005; Riley et al., 2013).

The limited number of post-fire erosion events documented in the study region makes somewhat problematic the understanding of the triggering factors or predisposing conditions controlling post-fire erosion responses. In volcaniclastic settings, not far from the study area, Calcaterra et al. (2007) and De Vita et al. (1994) documented that different post-fire geomorphic processes (e.g. landslides and debris flows) may occur in similar landscapes, also causing fatalities.

5.2 Post-fire soil loss

The soil erosion intensity map of Fig. 9 shows the areas involved by the post-fire response and the artificial channel at the outlet of the watershed. On the basis of the interpolation of fieldwork data, as a first step, we have inferred the volumes involved by erosion and subsequent depositional processes. Secondly, we have derived the soil loss per unit area at the watershed scale.

The balance between eroded and deposited sediments highlights a net excess of 58 tons of eroded material. This material was ostensibly redistributed along the hillslope and/or washed away from the channel by overland flows as suspended sediments. Since there was no significant evidence of erosion and instability processes in the unburned parts of the watershed, the burned sector can be regarded as the primary source area for the gravity flow deposits that accumulated in the concrete channel downstream.

Different estimates of the average post-fire soil loss can be obtained by dividing in turn the dry weight of channel deposits (218 tons), total deposited sediments (including hillslope and channel deposits, 306 tons) and eroded materials (364 tons) for the burned area (11 ha), resulting in a soil loss of 19.8, 27.8 and 33.1 tons ha^{-1}, respectively. This tendency to soil loss in the sediment budgets may be the result of larger scale entrapment of thin layers of material mobilized along the slopes, and/or by the dominance of hillslope processes over base of slope (channel) processes. Apparent soil loss in the system may also result from the occurrence of significant volumes of sediment or debris stored in the channel network, prior to the wildfire event.

The problem of soil loss during post-fire response events has been long debated in the literature. Shakesby (2011) reports values ranging between 0.016 and 13.1 tons ha^{-1} during the first year after wildfire for Mediterranean regions and 2.5 to 197 tons ha^{-1} in the USA and Australia. The case of Sant'Angelo Creek watershed seems in good agreement with annual erosion data collected at the catchment scale of the Mediterranean area and with figures documented in other regions after specific events (e.g. Copeland, 1965; Shakesby and Doerr, 2006; Moody and Martin, 2009; Lavabre and Martin, 1997; Robichaud et al., 2013). For example, Robichaud et al. (2013) reported soil losses of 18.6 tons ha^{-1} and 24.4 tons ha^{-1} after two short-duration high-intensity rainstorms (10-min maximum rainfall intensity respectively of 52 mm/h and 65 mm/h) in a 4.6-ha watershed in Colorado. Similarly, Copeland (1965) reported a soil loss of 9.6 tons ha^{-1} in a 98-ha watershed, in Nevada, during a rainstorm that reached a 5-min maximum rainfall intensity of 234.7 mm/h.

The methodological approaches of various authors and the different size of the burned areas represents one of the main problems in the calculation of soil loss within burned landscapes (Shakesby and Doerr, 2006; Moody and Martin, 2009). In this study, the calculated soil loss seems to be consistent both with the abundance of highly erodible

volcaniclastic soils mantling the carbonate slopes and with the moderate and high soil burn severity of the Sant'Angelo Creek watershed event.

The volcanic soils of study area, indeed, are very different from the typical thin and stony soils of the Mediterranean regions whose thickness is normally up to 35-50 cm (Shakesby, 2011). The soils involved by the Sant'Angelo creek fire are mainly 0.5 – 2.0 m thick (Fig. 2) and typically cohesionless (Damiano and Olivares, 2010). As a consequence, the shear strength of the topsoil horizons is significantly dependent by the occurrence of plant roots, as quantified by Nyman et al. (2013) for non-cohesive burned soils in Australia and United States.

Moreover, the role played by the vegetation is fundamental in reducing the kinetic energy of the raindrops and generating a mulch layer that prevents soil desiccation in low-rainfall periods. Therefore, we infer that in the study area, the burning of vegetation and litter cover caused by the wildfire resulted in effective erosion and transportation of fine sediment along the slopes.

According to Shakesby (2011), fire severity represents a key factor in controlling the degree of post-fire erosion. The Sant'Angelo creek event was characterized by moderate and high soil burn severity (35% and 65% respectively). According to our interpretation the fire had caused a significant decrease in the aggregate stability within the topsoil that likely reduced the critical shear stress required for the initiation of erosional processes (Moody and Smith, 2005; Mataix-Solera et al., 2011). According to Nyman et al. (2013), high severity wildfires can produce a hit pulse penetrating deeper into the soil than low-severity wildfires, and this may increase the corresponding depth of non-cohesive layer.

Based on the above observations we suggest that these factors, combined with the morphology of Sant'Angelo creek watershed and the intensity of the rainstorm event discussed in this study, have produced significantly high erosion and large volumes of sediments transported by overland flows downstream.

6 Conclusions

The data presented in this study document cause - effect relationship between the Sant'Angelo Creek fire (4 August, 2012) and the subsequent (6 September, 2012) post-fire erosion response. The event was triggered by a convective high-intensity and short-duration rainstorm that generated soil and sediment mass movements along the Sant'Angelo Creek watershed.

Erosion over the slopes was primarily driven by the entrainment of material due to runoff during post-fire erosion responses, and evolved with different magnitudes, mostly depending on slope morphology, vegetation cover and rain intensity. Quantitative analysis of sediment budgets showed that the Sant'Angelo Creek response caused a soil loss of about 19.8 to 33.1 tons ha^{-1} in the burned zone.

The results of this research suggest that wildfires can play a significant role in the geomorphological evolution of mountainous landscapes of the southern Apennines and similar contexts of the central Mediterranean area, especially when associated with heavy rainfall events. However, the lack of documented post-fire erosion responses, as well as inadequate knowledge about fire effects on volcanic soils of this geographic area, represent important issues. In order to better post-fire erosion mitigation strategies or emergency-response planning, future efforts to fill these research gaps are therefore essential.

Acknowledgements

This research work has been partly carried out during a CNR Short Term Mobility (STM) program conducted by G. Esposito at the USGS, Golden (CO), USA.

Thanks are due to S. Cannon, D. Staley, J. Coe, D. Martin, J. Moody and B. Ebel for fruitful discussions and precious comments on fire-related processes and to J. Kean for the review of an early version of the manuscript. Analyses on soil and rock samples were conducted with the precious support of M. Capodanno in the sedimentological laboratory of the IAMC-CNR Institute, Napoli.

We gratefully thank Luciano Cortese and Fernando Stanzione for SEM, XRD and ICP analyses. We also acknowledge the Civil Protection Department of Campania Region for allowing us access to rainfall data on the study area for the period August - September 2012 as well as the State Forestry Corps of Sarno for providing us information on wildfires in the study area, and Municipality of Sarno for providing us the DTM of the study area.

Financial support was provided by the Research Project PON-MONICA (contract n° PON01_01525) and the 2013 CNR STM Program.

References

Arca, B., Pellizzaro, G., Duce, P., 2010. Climate change impact on fire probability and severity in Mediterranean areas, in: Proceedings of the "VI International Conf. on Forest Fire Research", Coimbra, Portugal, 15-18 November 2010.

ASTM D-5142, 1996. Standard Test Methods for Proximate Analysis of the Analysis Sample of Coal and Coke by Instrumental Procedures. ASTM Book of Standards Vol. 05.05, West Conshohocken, PA.

ASTM Standard D-854, 2010. Specific Gravity of Soil Solid by Water Pycnometer. ASTM International West Conshohocken, PA.

Autorità di Bacino del Sarno, 2011. Piano Stralcio di Bacino per l'Assetto Idrogeologico – Carta degli spessori delle coperture piroclastiche in scala 1:5000, Napoli, Italy.

Beguería, S., 2006. Changes in land cover and shallow landslide activity: a case study in the Spanish Pyrenees. Geomorphology 74, 196–206.

Bertrand, N., Desgranges, C., Poquillon, D., Lafont, M.C., Monceau, D., 2010. Iron Oxidation at Low Temperature (260–500 C) in Air and the Effect of Water Vapor. Oxidation of Metals 73, 39–162.

Bisdom, E.B.A., Dekker, L.W., Schoute, J.F.T., 1993. Water repellency of sieve fractions from sandy soils and relationships with organic material and soil structure. Geoderma 56, 105-118.

Blake, W.H., Theocharopoulos, S.P., Skoulikidis, N., Clark, P., Tountas, P., Hartley, R., Amaxidis, Y., 2010. Wildfire impacts on hillslope sediment and phosphorus yields. Journal of Soils and Sediments 10, 671-682.

Calcaterra, D., Parise, M., Strumia, S., Mazzella, E., 2007. Relations between fire, vegetation and landslides in the heavily populated metropolitan area of Naples, Italy,

in: Proceedings 1st North American Landslides Conference, Vail, Colorado. AEG Special Publication 23, pp. 1448-1461.

Cannon, S.H., Bigio, E.R., Mine, E., 2001. A process for fire-related debris flow initiation, Cerro Grande fire, New Mexico. Catena 70, 396-409.

Cannon, S.H., DeGraff, J.D., 2009. The increasing wildfire and post-fire debris-flow threat in Western USA, and implications for consequences of climate change, in: Sassa K, Canuti P (eds) Landslides—disaster risk reduction. Springer, Berlin Heidelberg, pp. 177–190.

Cannon, S.H., Gartner, J.E., Holland-Sears, A., Thurston, B.M., Gleason, J.A., 2003a. Debris-flow response of basins burned by the 2002 Coal Seam and Missionary Ridge fires, Colorado, in: Boyer, D.D., Santi, P.M., Rogers, W.P. (Eds.), Engineering Geology in Colorado Contributions, Trends, and Case Histories. AEG Special Publication 15.

Cannon, S.H., Gartner, J.E., Parrett, C., Parise, M., 2003b. Wildfire-related debris flow generation through episodic progressive sediment bulking processes, western U.S.A, in: Rickenmann, D., Chen, C.L. (Eds.), Debris-Flow Hazards Mitigation: Mechanics, Prediction, and Assessment. Millpress, Rotterdam, in: Proceedings 3rd International DFHM Conference, Davos, Switzerland, pp. 71-82.

Cannon, S.H., Powers, P.S., Savage, Z., 1998. Fire-related debris flows on Storm King Mountain, Glenwood Springs, Colorado, USA. Environmental Geology 35, 210–218.

Cascini, L., Sorbino, G., Cuomo, S., 2003. Modelling of flowslides triggering in pyroclastic soils, in: Fasl Slope Movements Prediction and Prevention for Risk Mitigation, pp. 93-100. Bologna, PATRON. ISBN:8855526995

Cascini, L., Cuomo, S., Guida, D., 2008. Typical source areas of May 1998 flow-like mass movements in the Campania region, Southern Italy. Engineering Geology 96(3), 107-125.

Cascini, L., Sorbino, G., Cuomo, S., Ferlisi, S., 2013. Seasonal effects of rainfall on the shallow pyroclastic deposits of the Campania region (southern Italy). Landslides 11, 779-792.

Certini, G., 2005. Effects of fire on properties of forest soils: a review. Oecologia 143, 1–10.

Ciervo, F., Medina, V., Papa, M.N., Bateman, A., 2012. Reconstruction and numerical modelling of a flash flood event: Atrani 2010, In: Proceedings of the International workshop on flash flood and debris flow risk management in Mediterranean areas, Salerno, Italy, p. 21.

Copeland, O.L., 1965. Land use and ecological factors in relation to sediment yields, in: Proceedings of Federal Interagency Sedimentation Conference, 1963: U.S. Dept. Agriculture Misc. Pub. 970, pp. 72-84

Damiano, E., Olivares, L., 2010. The role of infiltration processes in steep slope stability of pyroclastic granular soils: Laboratory and numerical investigation. Natural Hazards 52, 329-350.

DeBano, L.F., 2000. The role of fire and soil heating on water repellency in wildland environments: a review. Journal of Hydrology 231–232, 195–206.

DeBano, L.F., 1981. Water repellent soils: a state of the art. USDA Forest Service General Technical Report PS W-46.

De Luca, C., Furcolo, P., Rossi, F., Villani, P., Vitolo, C., 2010. Extreme rainfall in the Mediterranean, in: Proceedings of the International Workshop on Advances in statistical hydrology, Taormina, Italy.

http://www.risorseidriche.dica.unict.it/Sito_STAHY2010_web/proceedings.htm (accessed 10.1.16).

De Santis, F., Giannossi, M.L., Medici, L., Summa, V., Tateo, F., 2010. Impact of physico-chemical soil properties on erosion features in the Aliano area (Southern Italy). Catena 81, 172-181.

De Vita, P., Napolitano, E., Godt, J., Baum, R., 2013. Deterministic estimation of hydrological thresholds for shallow landslide initiation and slope stability models: case study from the Somma-Vesuvius area of southern Italy. Landslides 10, 713-728.

De Vita, P., Celico, P., Siniscalchi, M., Panza, R., 2006. Distribution, hydrogeological features and landslide hazard of pyroclastic soils on carbonate slopes in the area surrounding Mount Somma-Vesuvius (Italy). Italian Journal of Engineering Geology and Environment 1, 75–98.

De Vita, P., Guadagno, C., Lanzara, R., Lombardi, G., Tarantino, E., Vallario, A., 1994. L'evento alluvionale del 20 agosto 1993 nei territori comunali di Solofra e Serino (Avellino - Campania), in: Atti VIII Congresso Nazionale Geologi, Roma, Italy, pp. 165-171.

Di Nocera, S., Matano, F., Pescatore, T., Pinto, F., Torre, M., 2011. Geological Characteristics of the External Sector of the Campania-Lucania Apennines in the CARG Maps. Rendiconti Online della Società Geologica Italiana 12, 39-43.

Ducci, D., Tranfaglia, G., 2008. The Effect of Climate Change on the Hydrogeological Resources in Campania Region (Italy), in: Dragoni, W., Sukhija, B.S. (Eds.), Climatic

changes and Groundwater. Geological Society, Special Publications 288, London, pp. 25-38.

Esposito, E., Porfido, S., Tranfaglia, G., Iaccarino, G., Esposito, G., Braca, G., 2004. Correlation between pluviometric data and sliding phenomena in Naples, Southern Italy. Atti dei convegni lincei - accademia nazionale dei lincei 181, 379-386.

Esposito, G., Esposito, E., Matano, F., Molisso, F., Porfido, S., Sacchi, M., 2013. Effects of a wildfire on rocks and soils in the Sarno Mountains, Campania, Southern Apennines. Rendiconti Online della Società Geologica Italiana 24, 119-121.

Esposito, G., Fortelli, A., Grimaldi, M.G., Matano, F., Sacchi, M., 2015. I fenomeni di flash flood nell'area costiera di Pozzuoli (Napoli, Italia): risultati preliminari sull'analisi dell'evento del 6 novembre 2011. Rendiconti Online della Società Geologica Italiana 34, 74-84.

Farres, PJ., 1987. The dynamics of rainsplash erosion and the role of soil aggregate stability. Catena 14, 119-130.

Folk, R.L., 1974. Petrology of Sedimentary Rocks. Hemphill Publishing Company, Austin, 182.

Folk, R.L., Ward, W.C., 1957. Brazos river bar: a study of significante of grain size parameters. Journal of Sedimentary Petrology 27, 3-26.

García-Ruiz, J.M., Arnáez, J., Gómez-Villar, A., Ortigosa, L., Lana-Renault, N., 2013. Fire-related debris flows in the Iberian Range, Spain. Geomorphology 196, 221-230.

García-Ruiz, J.M., Beguería, S., Alatorre, L.C., Puigdefábregas, J., 2010. Land cover changes and shallow landsliding in the Flysch Sector of the Spanish Pyrenees. Geomorphology 124, 250–259.

Gargiulo, L., Mele, G., Terribile, F., 2013. Image analysis and soil micromorphology applied to study physical mechanisms of soil pore development: An experiment using iron oxides and calcium carbonate. Geoderma 197-198, 151-160.

Gartner, J.E., Bigio, E.R., Cannon, S.H., 2005. Compilation of post wildfire runoff-event data from the Western United States. U.S. Geological Society Open-File Report 2004–1085. http://pubs.usgs.gov/of/2004/1085/ofr-04-1085.html (accessed 3.10.15).

Guadagno, F.M., Forte, R., Revellino, P., Fiorillo, F., Focareta, M., 2005. Some aspects of the initiation of debris avalanches in the Campania Region: The role of morphological slope discontinuities and the development of failure. Geomorphology 66, 237–254.

ISPRA (Istituto Superiore per la Protezione e la Ricerca Ambientale) – Servizio Geologico d'Italia, 1976. Geological map of Italy at 1:100,000 scale, Roma, Italy.

JRC - Joint Research Centre, 2015. Forest Fires in Europe, Middle East and North Africa 2014. http://forest.jrc.ec.europa.eu/effis/reports/annual-fire-reports/ (accessed 02.10.2016).

JRC - Joint Research Centre, 2013. Forest Fires in Europe, Middle East and North Africa 2012. http://forest.jrc.ec.europa.eu/effis/reports/annual-fire-reports/ (accessed 02.10.2016).

Jordàn, A., Zavala, L.M., Mataix-Solera, J., Doerr, S.H., 2013. Soil water repellency: Origin, assessment and geomorphological consequences. Catena 108, 1-5.

Jozefaciuk, G., Czachor, H., 2014. Impact of organic matter, iron oxides, alumina, silica and drying on mechanical and water stability of artificial soil aggregates: Assessment of new method to study water stability. Geoderma 221–222, 1–10.

Kean, J.W., McCoy, S.W., Tucker, G.E., Staley, D.M., Coe, J.A., 2013. Runoff-generated debris flows: Observations and modeling of surge initiation, magnitude, and frequency. Journal of Geophysical Research: Earth Surface 118, 2190-2207.

Kean, J.W., Staley, D.M., Cannon, S.H., 2011. In situ measurements of post-fire debris flows in southern California: Comparisons of the timing and magnitude of 24 debris-flow events with rainfall and soil moisture conditions. Journal of Geophysical Research 116, F04019.

Lavabre, J., Martin, C., 1997. Impact d'un incendie de forêt sur l'hydrologie et l'érosion hydrique d'un petit bassin versant méditerranéan. Human Impact on Erosion and Sedimentation, in: Proceedings of Rabat Symposium S6, April 1997, IAHS Publication 245, pp. 39-47.

Le Bissonnais, Y., Bruand, A., Jamagne, M., 1989. Laboratory experimental study of soil crusting: relation between aggregate breakdown mechanisms and crust structure. Catena 16, 377-392.

Lorente, A., Beguería, S., Bathurst, J.C., García-Ruiz, J.M., 2003. Debris flow characteristics and relationships in the Central Spanish Pyrenees. Natural Hazards and Earth System Sciences 3, 683–692.

Lorente, A., García-Ruiz, J.M., Beguería, S., Arnáez, J., 2002. Factors explaining the spatial distribution of hillslope debris flows. A case study in the Flysch Sector of the Central Spanish Pyrenees. Mountain Research and Development 22, 32–39.

Lourenço, L., Nunes, A.N., Bento-Gonçalves, A., Vieira, A., 2012. Soil erosion After Wildfires in Portugal: What Happens When Heavy Rainfall Event Occur?, in: Danilo Godone, Silvia Stanchi (Ed.), Research on Soil Erosion, InTech, ISBN: 978-953-51-0839-92.

Maeda, T., Takenaka, H., Warkentin, B.P., 1977. Physical properties of allophane soils. Advances in Agronomy 29, 229-264.

Mataix-Solera, J., Cerdà, A., Arcenegui, V., Jordán, A., Zavala, L.M., 2011. Fire effects on soil aggregation: a review. Earth-Science Reviews 109, 44-60.

Matano, F., De Chiara, G., Ferlisi, S., Cascini, L., 2016. Thickness of pyroclastic cover beds: the case study of Mount Albino (Campania region, southern Italy). Journal of Maps 12, 79-87.

McGuire, L.A., Kean, J.W., Staley, D.M., Rengers, F.K., Wasklewicz, T.A., 2016. Constraining the relative importance of raindrop- and flow-driven sediment transport mechanisms in postwildfire environments and implications for recovery time scales, Journal of Geophysical Research: Earth Surface 121, 1-27.

Meyer, G.A., Wells, S.G., 1997. Fire-related sedimentation events on alluvial fans, Yellowstone National Park, U.S.A. Journal of Sedimentary Research 67, 776-79.

Moody, J.A., Shakesby, R.A., Robichaud, P.R., Cannon, S.H., Martin, D.A., 2013. Current research issues related to post-wildfire runoff and erosion processes. Earth-Science Reviews 122, 10-37.

Moody, J.A., Martin, D.A., 2009. Synthesis of sediment yields after wildland fire in different rainfall regimes in the western United States. International Journal of Wildland Fire 18, 96-115.

Moody, J.A., Smith, J.D., 2005. Critical shear stress for erosion of cohesive soils subjected to temperatures typical of wildfires. Journal of Geophysical Research 110, 1-13.

Moriondo, M., Good, P., Durao, R., Bindi, M., Giannakopoulos, C., Corte-Real, J., 2006. Potential impact of climate change on fire risk in the Mediterranean area. Climate Research 13, 85-95.

Morris, R., Buckman, S., Connelly, P., Dragovich, D., Ostendorf, B., Bradstock, R., 2011. The dirt on assessing post-fire erosion in the Mount Lofty Ranges: comparing methods, in: Proceedings of Bushfire CRC & AFAC 2011 Conference Science Day, Sydney, Australia, pp. 152-169.

Munsell Soil Color Charts., 1994. New Windson: Kollmorgen Instruments-Macbeth Division.

Neris, J., Santamarta, J.C., Doerr, S.H., Prieto, F., Agulló-Pérez, J., Garcìa-Villegas, P., 2016. Post-fire soil hydrology, water erosion and restoration strategies in Andosols: a review of evidence from the Canary Islands (Spain). iForest - Biogeosciences and Forestry (early view), e1-e10.

Nyman, P., 2013. Post-fire debris flows in southeast Australia: initiation, magnitude and landscape controls. PhD thesis, Melbourne School of Land and Environment, The University of Melbourne.

Nyman, P., Smith, H.G., Sherwin, C.B., Langhans, C., Lane, P.N.J., Sheridan, G.J., 2015. Predicting sediment delivery from debris flows after wildfire. Geomorphology 250, 173-186.

Nyman, P., Sheridan, G. J., Smith, H. G., Lane, P. N. J., 2011. Evidence of debris flow occurrence after wildfire in upland catchments of south-east Australia. Geomorphology 125, 383-401.

Nyman, P., Sheridan, G.J., Moody, J.A., Smith, H.G., Noske, P.J., Lane, P.N.J., 2013. Sediment availability on burned hillslopes. Journal of Geophysical Research: Earth Surface 118, 2451-2467.

Orsi, G., De Vita, S., Di Vito, M., 1996. The restless, resurgent Campi Flegrei Nested Caldera (Italy): Constraints on its evolution and configuration. Journal of Volcanology and Geothermal Research 74, 179–214.

Parise, M., Cannon, S., 2008. The effects of wildfires on erosion and debris-flow generation in Mediterranean climatic areas: a first database, in: Proceedings of 1st World Landslide Forum, Tokyo, Japan, pp. 465-468.

Parsons, A., Robichaud, P.R., Lewis, S.A., Napper, C., Clark, J.T., 2010. Field guide for mapping post-fire soil burn severity. USDA Forest Service, Fort Collins, Colorado, General Technical Report RMRS-GTR-243.

Pelletier, J.D., Orem, C.A., 2014. How do sediment yields from post-wildfire debris-laden flows depend on terrain slope, soil burn severity class, and drainage basin area? Insights from airborne-LiDAR change detection. Earth Surface Processes and Landforms 39, 1822-1832.

Pierson, T.C., 2005. Hyperconcentrated flow-transitional process between water flow and debris flow, in: Jakob, M., Hungr, O. (Eds.), Debris-flow Hazards and Related Phenomena. Springer/Praxis, Chichester (UK), pp. 159-202.

Pierson, T.C., Costa, J.E., 1987. A rheologic classification of subaerial sediment-water flows, in: Costa, J.E., Wieczorek, G.F. (Eds.), Debris flows/Avalanches: Process, Recognition, and Mitigation. Geological Society of America Reviews in Engineering Geology 7, pp. 1-12.

Porfido, S., Esposito, E., Alaia, F., Molisso, F., Sacchi, M., 2009. The use of documentary sources for reconstructing flood chronologies on the Amalfi rocky coast (southern Italy), in: Violante, C. (Eds.), Geohazard in Rocky Coastal Areas. Geological Society, Special publication 322, London, pp. 173–187.

Prosser, I., Williams, L., 1998. The effect of wildfire on runoff and erosion in native Eucalyptus forest. Hydrological Processes 12, 251–265.

Regelink, I.C., Stoof, C.R., Rousseva, S., Weng, L., Lair, G.J., Kram, P., Nikolaidis, N.P., Kercheva, M., Banwart, S., Comans, R.N.J., 2015. Linkages between aggregate formation, porosity and soil chemical properties. Geoderma 247-248, 24-37.

Regional Department of Agriculture, 2013. Piano antincedio boschivo 2013. http://www.agricoltura.regione.campania.it/comunicati/pdf/AIB_2013.pdf (accessed 02.10.2016)

Riley, K. L., Bendick, R., Hyde, K.D., Gabet, E.J., 2013. Frequency–magnitude distribution of debris flows compiled from global data, and comparison with post-fire debris flows in the western U.S. Geomorphology 191, 118-128.

Robertson, S., 2011. Direct Estimation of Organic Matter by Loss on Ignition: Methods. http://www.sfu.ca/soils/lab_documents/Estimation_Of_Organic_Matter_By_LOI.pdf (accessed 20.7.15).

Robichaud, P.R., Wagenbrenner, J.W., Lewis, S.A., Ashmun, L.E., Brown, R.E., Wohlgemuth PM. 2013. Post-fire mulching for runoff and erosion mitigation Part II: effectiveness in reducing runoff and sediment yields from small catchments. Catena 105, 93–111.

Robichaud, P.R., Brown, R.E., 2002. Silt fences: an economical technique for measuring hillslope soil erosion. U.S. Department of Agriculture, Forest Service, Rocky Mountain Research Station, Fort Collins, Colorado. Gen. Tech. Rep. RMRS-GTR-94.

Rodríguez, A., Guerra, J.A., Gorrín, S.P., Arbelo, C.D., Mora, J.L., 2002. Aggregates stability and water erosion in andosols of the Canary islands. Land Degradation & Development 13, 515-523.

Rolandi, G., Petrosino, P., McGeehin, J., 1998. The interplinian activity at Somma-Vesuvius in the last 3500 years. Journal of Volcanology and Geothermal Research 82, 19-52.

Rosso, R., Rulli, M.C., Bocciola, D., 2007. Transient catchment hydrology after wildfires in a Mediterranean basin: runoff, sediment and woody debris. Hydrology and Earth System Sciences 11(1), 125-140.

Rulli, M.C., Offeddu, L., Santini, M., 2013. Modeling post-fire water erosion mitigation strategies. Hydrology and Earth System Sciences 17, 2323-2337.

Rulli, M.C., Spada, M., Bozzi, S., Bocchiola, D., Rosso, R., 2006. Rainfall simulations on a fire disturbed Mediterranean area. Journal of Hydrology 327, 323-338.

Santi, P., Cannon, S., DeGraff, J., 2013. Wildfire and Landscape Change, in: Shroder, J. (Editor in Chief), James, L.A., Harden, C.P., Clague, J.J. (Eds.), Treatise on Geomorphology. Academic Press, San Diego, CA, Vol. 13, Geomorphology of Human Disturbances, Climate Change, and Natural Hazards, pp. 262–287.

Santo, A., Di Crescenzo, G., Del Prete, S., Di Iorio, L., 2012. The Ischia island flash flood of November 2009 (Italy): Phenomenon analysis and flood hazard. Physics and Chemistry of the Earth 49, 3–17.

Scott, K.M., 1988. Origins, behavior, and sedimentology of lahars and lahar-runout flows in theToutle-Cowlitz system. U.S. geol. Survey Prof. Paper 1447-A: 1-74.

Shakesby, R.A., 2011. Post-wildfire soil erosion in the Mediterranean: Review and future research directions. Earth-Science Reviews 105, 71-100.

Shakesby, R.A., Doerr, S.H., 2006. Wildfire as a hydrological and geomorphological agent. Earth-Science Reviews 74, 269–307.

Staley, D.M., Wasklewicz, T.A., Kean, J.W., 2014. Characterizing the primary material sources and dominant erosional processes for post-fire debris-flow initiation in a headwater basin using multi-temporal terrestrial laser scanning data. Geomorphology 214, 324-338.

Stefanidis, P., Sapountzis, M., Stathis, D. 2002. Sheet erosion after fire at the urban forest of Thessaloniki (Northern Greece). Silva Balcanica 2, 65-77.

Summa, V., Tateo, F., Medici, L., Giannossi, M.L., 2007. The role of mineralogy, geochemistry and grain size in badland development in Pisticci (Basilicata, Southern Italy). Earth Surface Processes and Landforms 32, 980-997.

Swanson, F.J., 1981. Fire and geomorphic processes, in: Mooney, H.A., Bonnicksen, T.M., Christiansen, N.L., Lotan, J.E., Reiners, W.A. (Eds.), Fire Regime and Ecosystem Properties. United States Department of Agriculture, Forest Service, General Technical Report WO, 26, United States Government Planning Office, Washington DC, pp. 401–421.

Terribile, F., Basile, A., De Mascellis, R., Iamarino, M., Magliulo, P., Pepe S., Vingiani S., 2007. Landslide processes and Andosols: the case study of the Campania region Italy, in: Arnalds, et al. (Eds.), Soils of Volcanic Regions in Europe. Springer-Verlag, Berlin, pp. 545-563.

Tiranti, D., Moscariello, A., Giudici, I., Rabuffetti, D., Cremonini, R., Campana, V., Bosco, F., Giardino, M., 2006. Post-fire rainfall events influence on debris-flows trigger mechanisms, evolution and sedimentary processes: the Rio Casella case study in the North-western Italian Alps, in: EGU General Assembly 2006 Geophysical Research Abstracts, Vol. 8, 03479, 2006 SRef-ID: 1607-7962/gra/EGU06-A-03479 © European Geosciences Union 2006.

Tranfaglia, G., Braca, G., 2004. Analisi idrologica e meteorologica dell'evento alluvionale del 24–25 Ottobre 1954: confronto con le serie storiche e valutazione del periodo di ritorno di eventi analoghi, in: Esposito, E., Porfido, S., Violante, C. (Eds.), Il nubifragio dell'Ottobre 1954 a Vietri sul mare. Costa d'Amalfi, Salerno. Pubblicazione G.N.D.C.I. n. 2870, pp. 295–348.

US Environmental Protection Agency (EPA) Method 3051, 1998. Microwave assisted acid digestion of sediments, sludge, soils and oils. January 1998. US EPA Office of Solid Waste. Washington D.C.

US Environmental Protection Agency (EPA) Method 3052, 1996. Microwave assisted acid digestion of siliceous and organically based matrices. December 1996. US EPA Office of Solid Waste. Washington D.C.

Vafeidis, A.T., Drake, N.A., Wainwright, J., 2007. A proposed method for modelling the hydrologic response of catchments to burning with the use of remote sensing and GIS. Catena 70, 396-409.

VanDine, D.F., Rodman, R.F., Jordan, P., Dupas, J., 2005. Kuskonook Creek, an example of a debris flow analysis. Landslides 2, 257-265.

Warkentin, B.P., 1984. Physical properties of forest-nursery soils: relation to seedling growth, in: Duryea ML, Landis TD, editors. Forest nursery manual: production of bareroot seedlings. Boston (MA): Martinus Nijhoff/Dr W Junk Publishers, pp. 53-62.

Wells, W.G., Wohlgemuth P.M., 1987. Sediment traps for measuring on slope surface sediment movement. USDA Forest Service, Berkeley, California. Research Note PSW-393.

Wondzell, S.M., King, J.G., 2003. Postfire erosional processes in the Pacific Northwest and Rocky Mountain regions. Forest Ecology and Management 178, 75–87.

WRB, 2006. World reference base for soil resources 2006. Reports, 103, FAO Press, Rome, Italy.

Web references

Crystallographic and Crystallochemical Database for Minerals and their Structural Analogues. http://database.iem.ac.ru/mincryst/index.php (accessed 1.2.16).

Weather forecast bulletin emitted by the Regional Civil Protection http://bollettinimeteo.regione.campania.it/?m=201209&paged=6 (accessed 5.1.16).

Tables

Parameters	Watershed	Burned area
area (ha)	55	11
perimeter (km)	3.343	1.610
slope min (°)	2	2
slope max (°)	58	54
slope range (°)	55.9	52
slope average (°)	34.9	34.8
alt min (m)	246	246
alt max (m)	891	560
relief ratio	0.45	--
main channel length (m)	1432	--
main channel slope (°)	23	--
main channel slope at outlet (°)	11	--

Table 1. Summary of some morphometric parameters related to the Sant'Angelo Creek watershed and to the burned area.

DEPTH (cm)	WDPT (s)							
	MODERATE SOIL BURN SEVERITY			HIGH SOIL BURN SEVERITY				
0	17	3	16	0	0	0	5	3
1	45	5	12	12	> 1900	10	25	18
2	15	18	39	160	> 1900	65	115	95
3	15	22	43	600	> 1900	150	348	110
4	18	38	41	> 1900	1536	800	> 1900	175
5	2	32	28	> 1900	1320	> 1900	> 1900	280
6	2	12	11	> 1900	10	> 1900	> 1900	1520
7	30	6	8	0	5	1200	> 1900	1568
8	10	4	5	0	2	22	10	1762
9	2	1	0	0	1	0	0	973
10	0	1	0	0	0	3	0	24

Table 2. WDPT test results performed in the areas burned with moderate and high soil burn severity.

RAIN GAUGE	RAINSTORM TIME INTERVAL (hours)	TOTAL STORM RAINFALL (mm)	I_{10} (mm/h)	I_{30} (mm/h)	DISTANCE FROM THE STUDY WATERSHED (km)
CETRONICO	04:50 - 6:30	23.8	37.2	30.8	4
BRACIGLIANO	04:50 - 6:20	22.2	37.2	25.2	4.4
PIANI DI PRATO	04:40 - 5:50	13.2	19.2	15.6	2.8

1

2 Table 3. Rainfall data collected by the Civil Protection rain gauges used in this study.

SAMPLE	TEXTURE	COLOR	% COMPONENTS (Phi-1÷1)			GRAIN SIZE PROPERTIES				G_s (g cm^{-3})	SOM (%)	W (%)	W_{AV} (%)
			Vege-table	*Vol-canic*	*Carbo-nate*	Mz (phi)	s (phi)	Sk (phi)	Kg (phi)				
B1	Gravelly muddy sand	Dark brown 10 YR 3/3	0 - 15	85 - 100	0	1.72	3.33	0.47	2.68	2.1	9.9	12	11.5
B2	Gravelly muddy sand	Brown 2.5 Y 3/2	< 5 - 10	90 - 95	0	2.42	3.32	0.29	2.11	2.3	8.4	11	
NB1	Gravelly muddy sand	Dark olive brown 2.5 Y 3/3	0 - 10	90 - 100	0	1.76	3.39	0.45	2.48	2.2	10.3	13	
NB2	Gravelly muddy sand	Dark grayish brown 2.5 Y 4/2	0 - 30	70 - 95	0-5	2.22	3.42	0.27	2.02	2.2	9.6	10	
D1	Muddy sandy gravel	Brown 2.5 Y 3/2	0	95	0-5	0.44	2.61	0.92	5.75	2.4	2.5	41	42
D2	Gravelly mud	Brown 2.5 Y 3/2	30 - 70	30 - 70	0	5.58	1.79	-0.56	4.92	1.9	27	43	

Table 4. Summary of the results obtained by laboratory analysis (Mz = mean particle size; s = sorting; Sk = skewness; Kg = Kurtosis; Gs = specific gravity; SOM = soil organic matter; W = water content; W_{AV} = average water content). Sample textures (Folk, 1974) are also indicated.

Element (ppm)	B1	NB1	B2	NB2
Aluminum	42660	42670	41740	44520
Barium	995	840	777	827
Calcium	18670	18550	18160	20160
Iron	19880	17540	18510	19770
Magnesium	7363	6659	7530	6928
Manganese	575.9	467.	526	546
Potassium	34770	31950	28770	27950
Sodium	9325	7574	6241	7346
Strontium	436	380	358	366
Titanium	1848	1448	1582	1677

Table 5. Amount of the inorganic elements measured in the burned and unburned soil samples.

Sample	Moisture (%)	Volatiles (%)	Ashes (%)	Fixed Carbon
B1	2.3	6.7	91.0	-
B2	2.6	8.6	88.4	0.44
NB1	2.2	6.6	91.2	-
NB2	3.1	9.0	87.9	1.4

Table 6. Proximate Analysis results

HIGHLIGHTS

- We describe a post-fire erosion response of a steep watershed in Italy.
- The fire burned 11 ha of forest with high and moderate severity.
- The erosion response was triggered by a convective rainstorm.
- A hyperconcentrated flow resulted from sediment bulking of surface runoff
- Amount of soil loss was estimated

Figure_1

Click here to download high resolution image

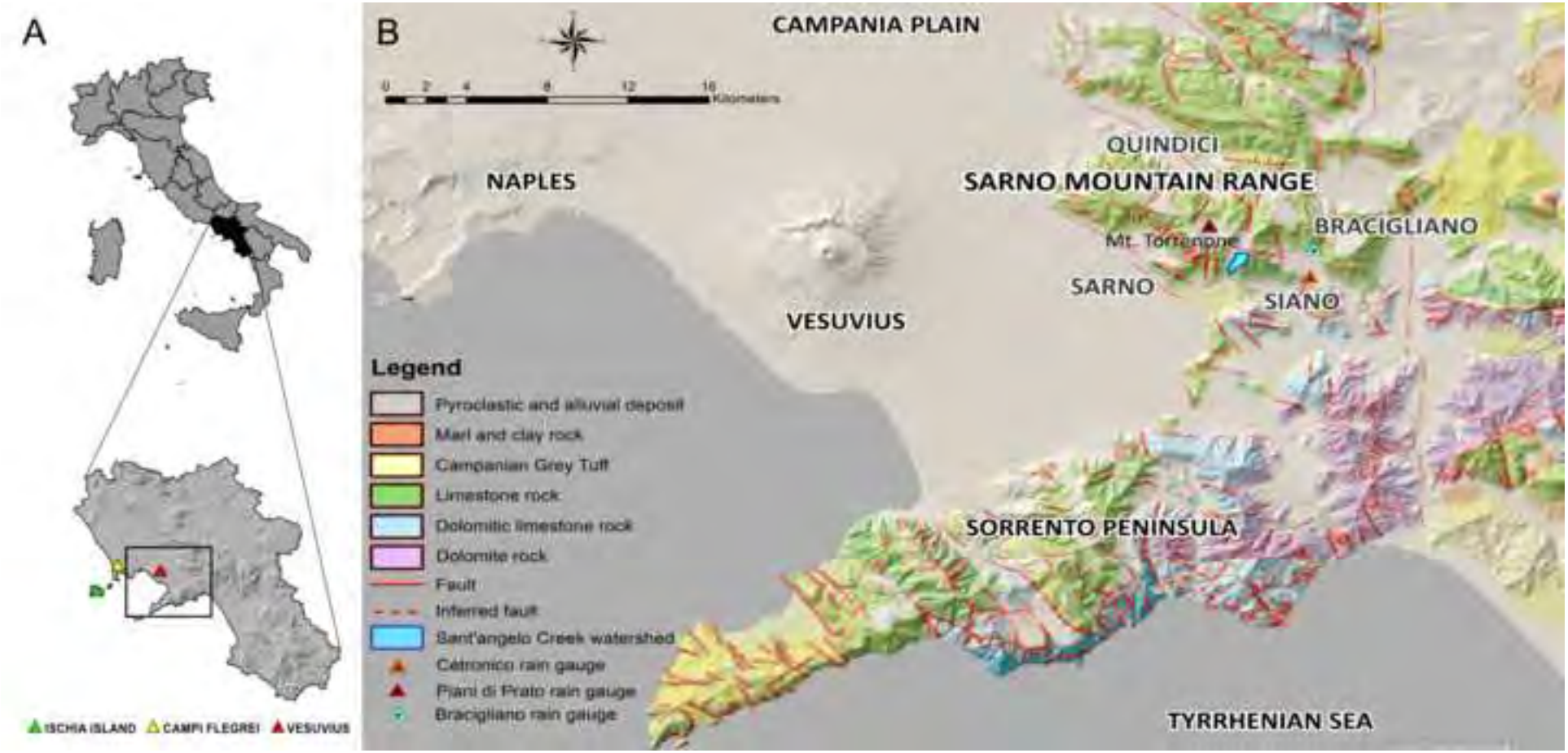

Figure_2

Click here to download high resolution image

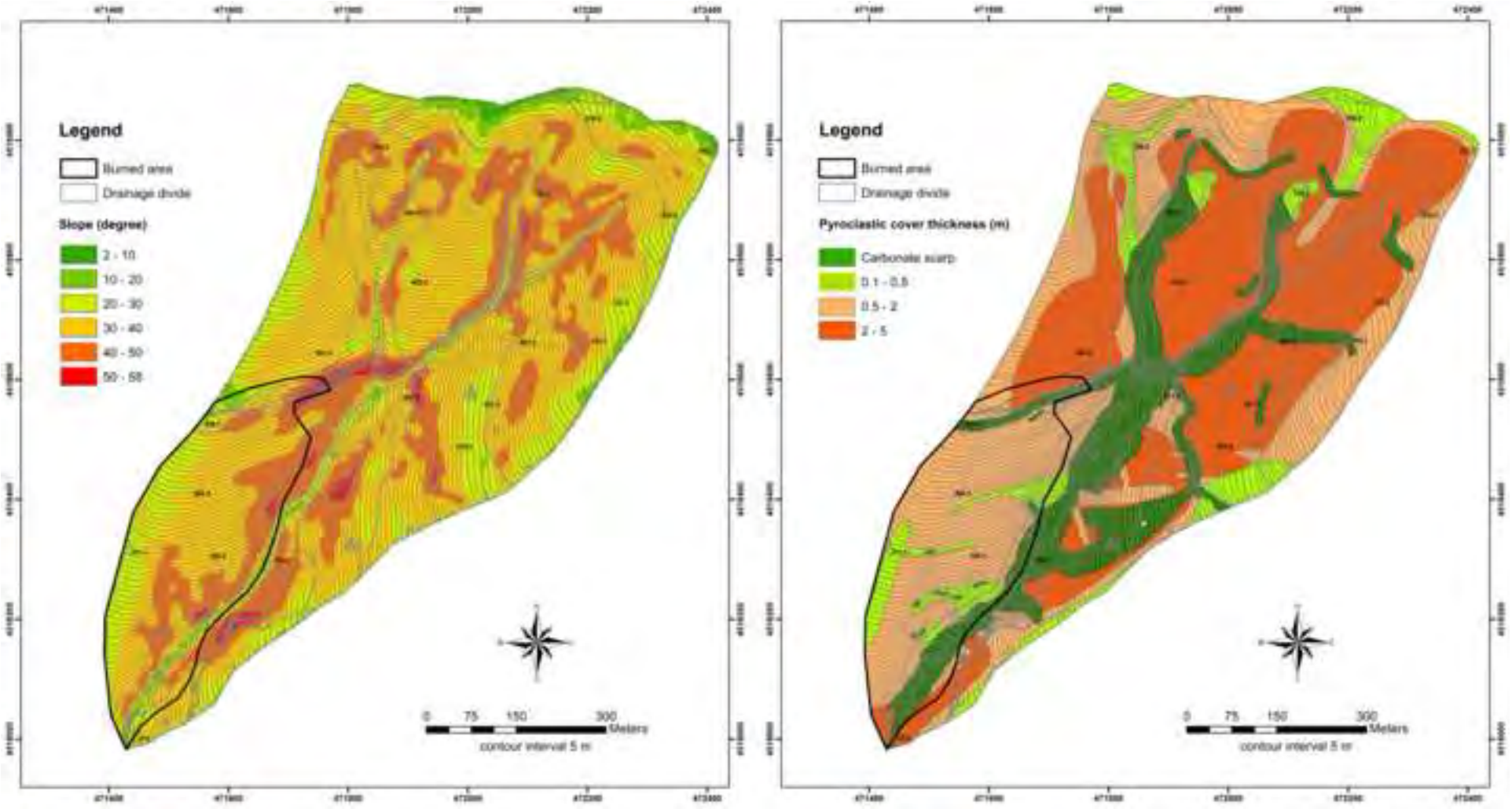

Figure_3

Click here to download high resolution image

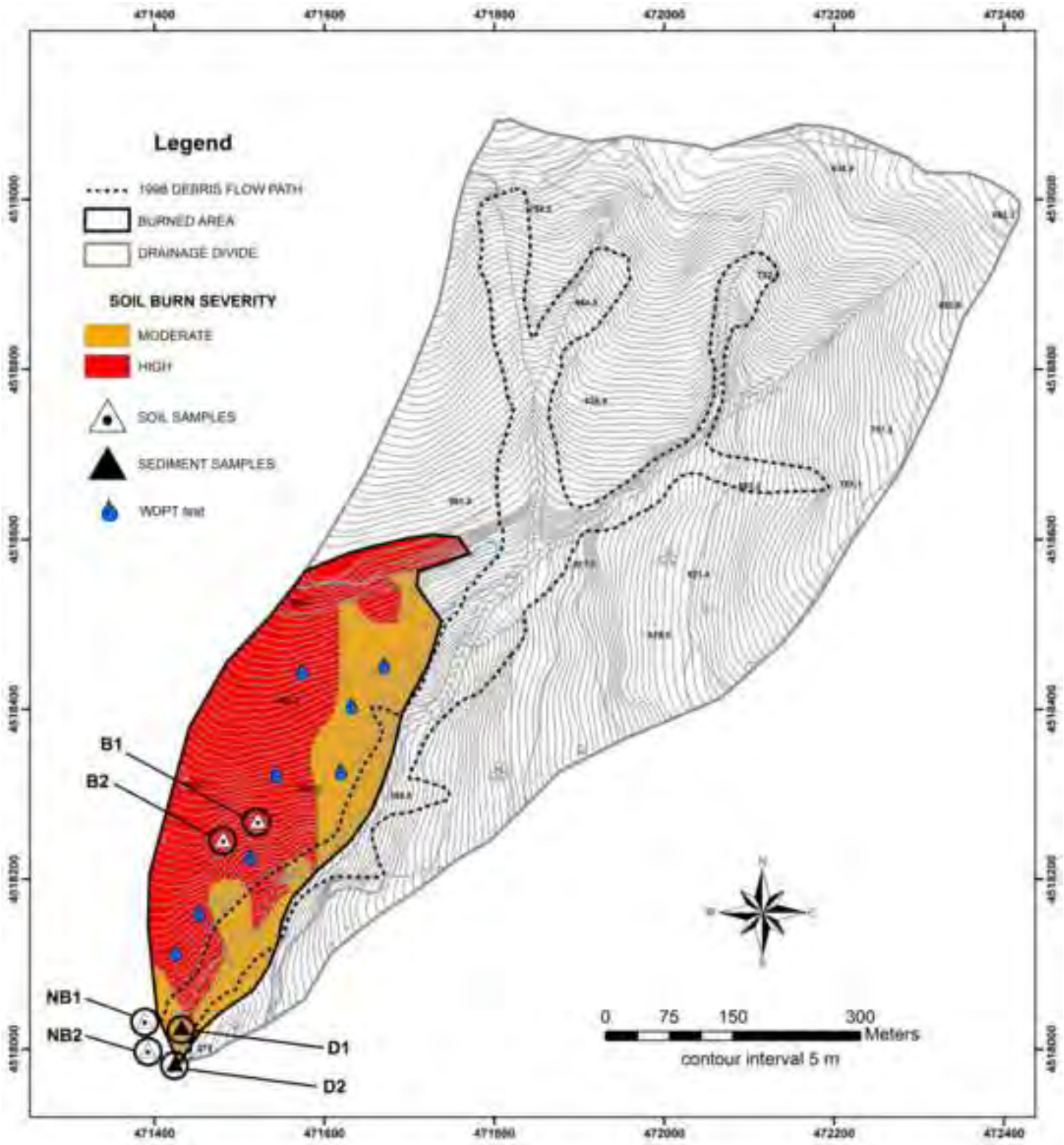

Figure_4
Click here to download high resolution image

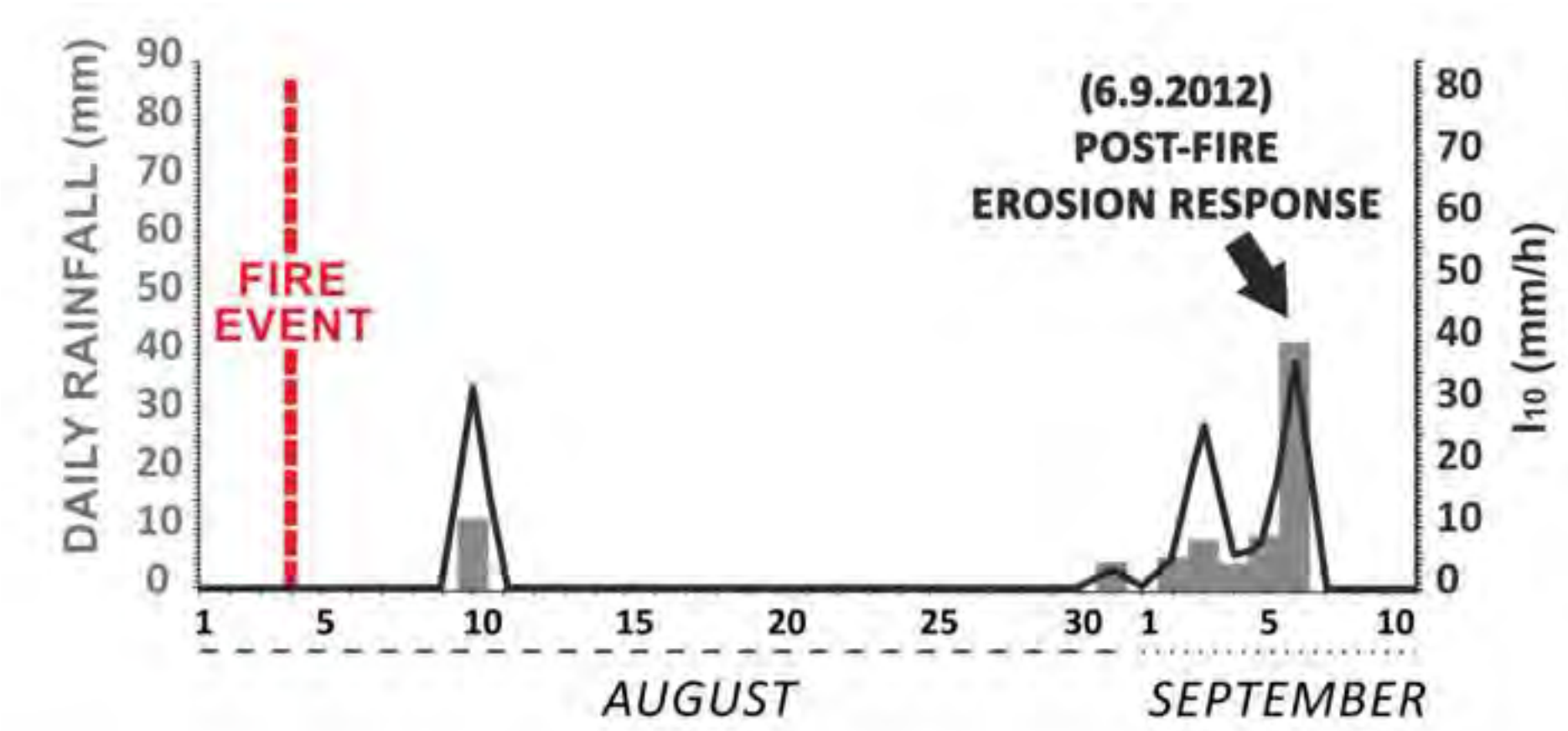

Figure_5

Click here to download high resolution image

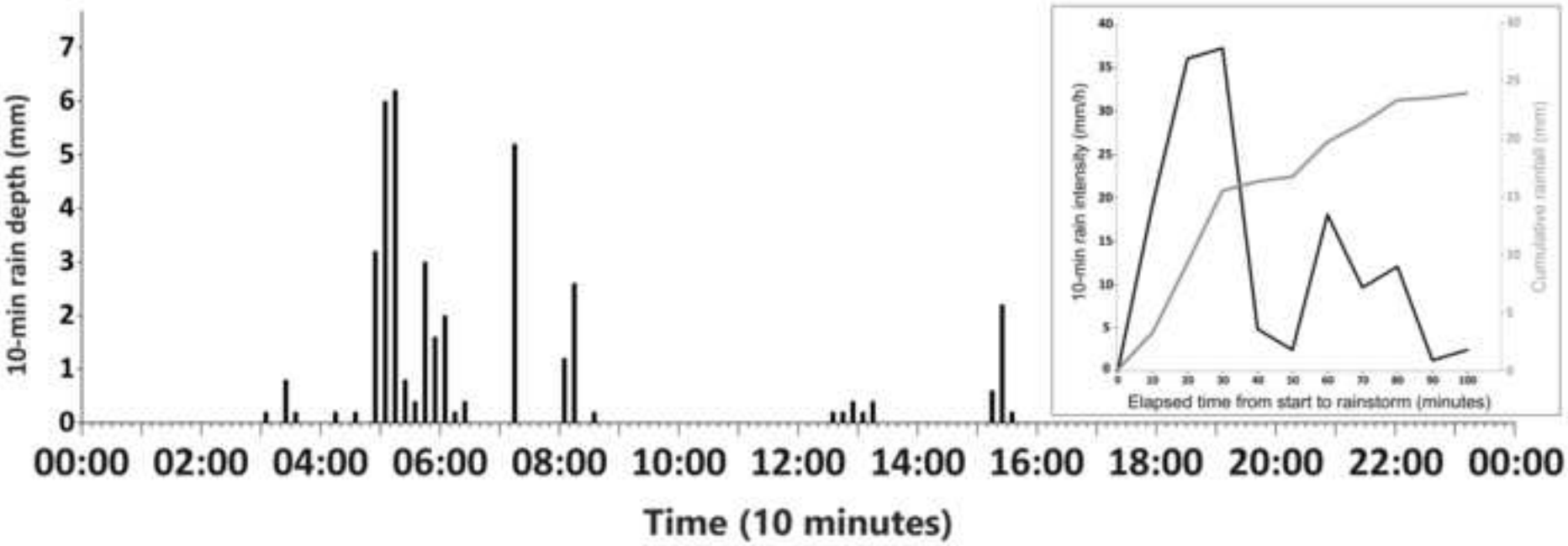

Figure_6
Click here to download high resolution image

Figure_7

Click here to download high resolution image

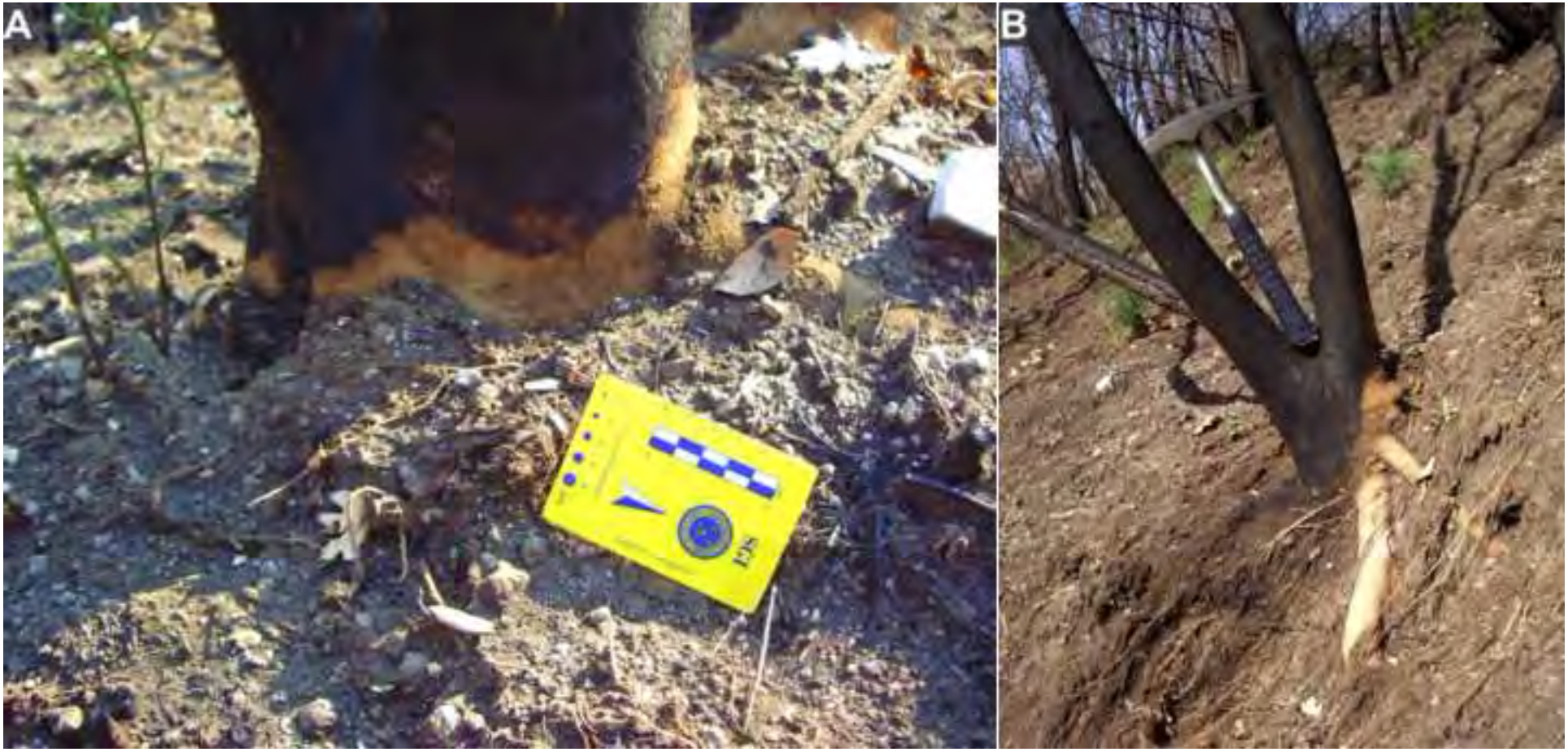

Figure_8
Click here to download high resolution image

Figure_9

Click here to download high resolution image

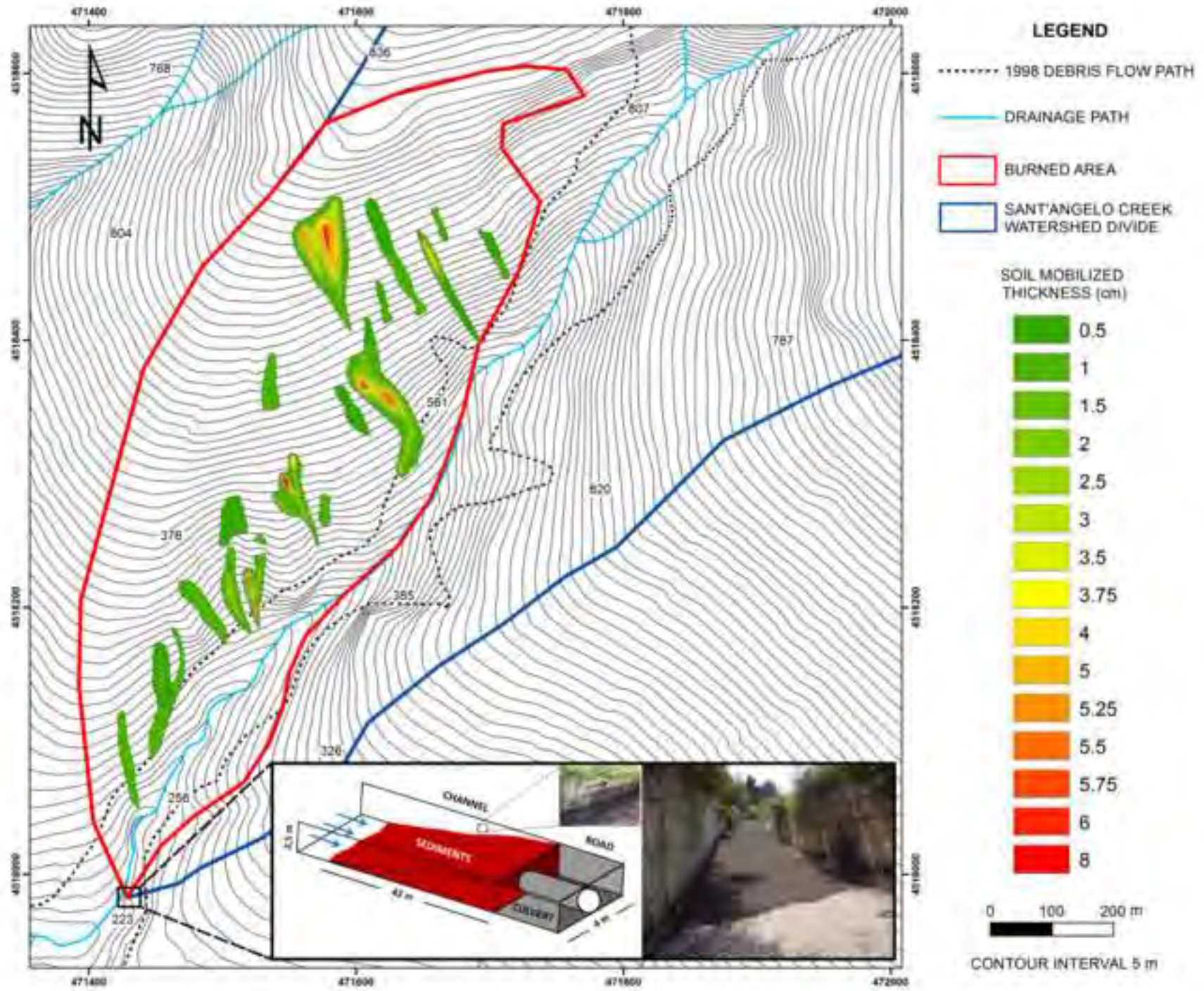

Figure_10
Click here to download high resolution image

Figure_11
Click here to download high resolution image

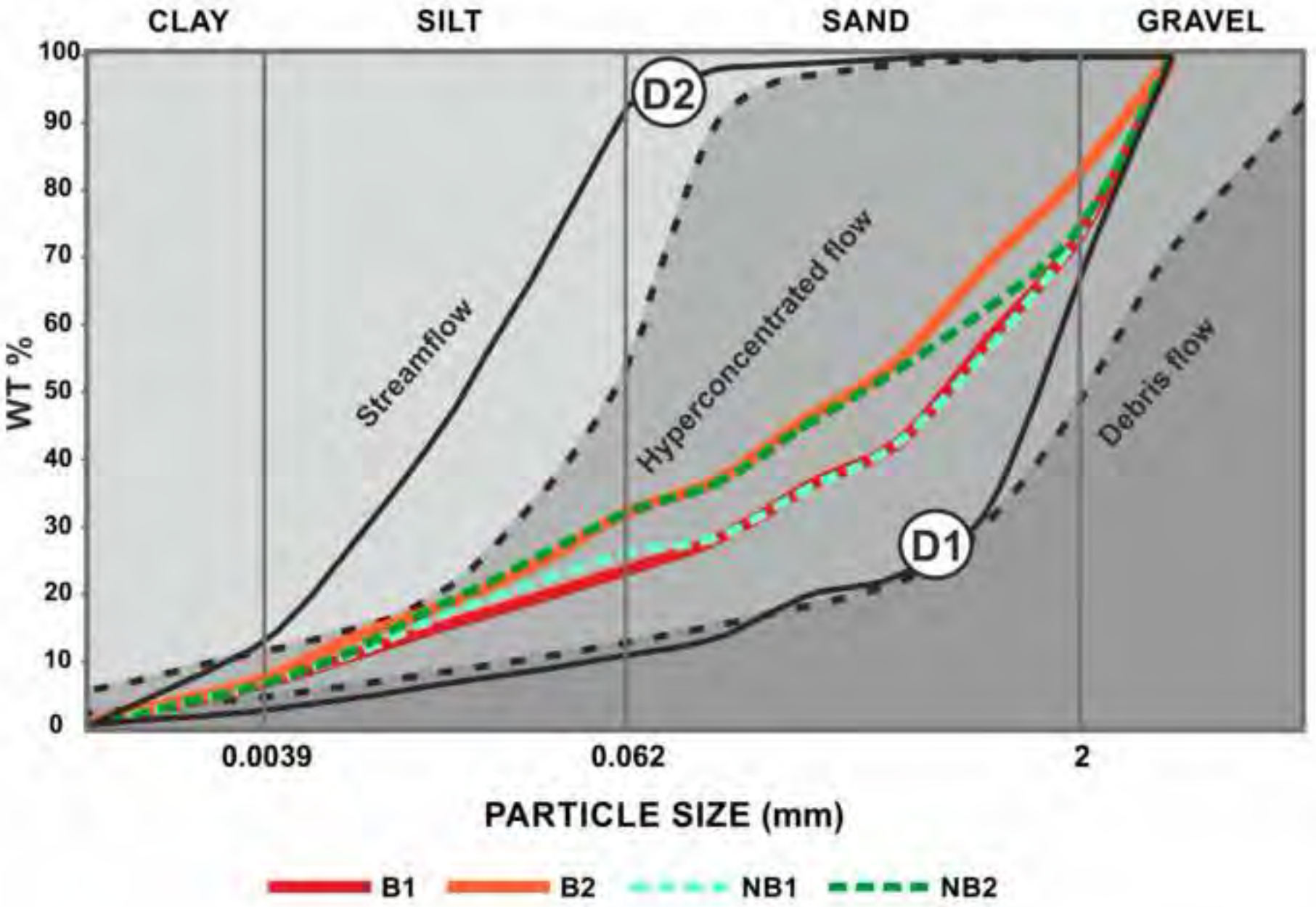

Figure_12
Click here to download high resolution image

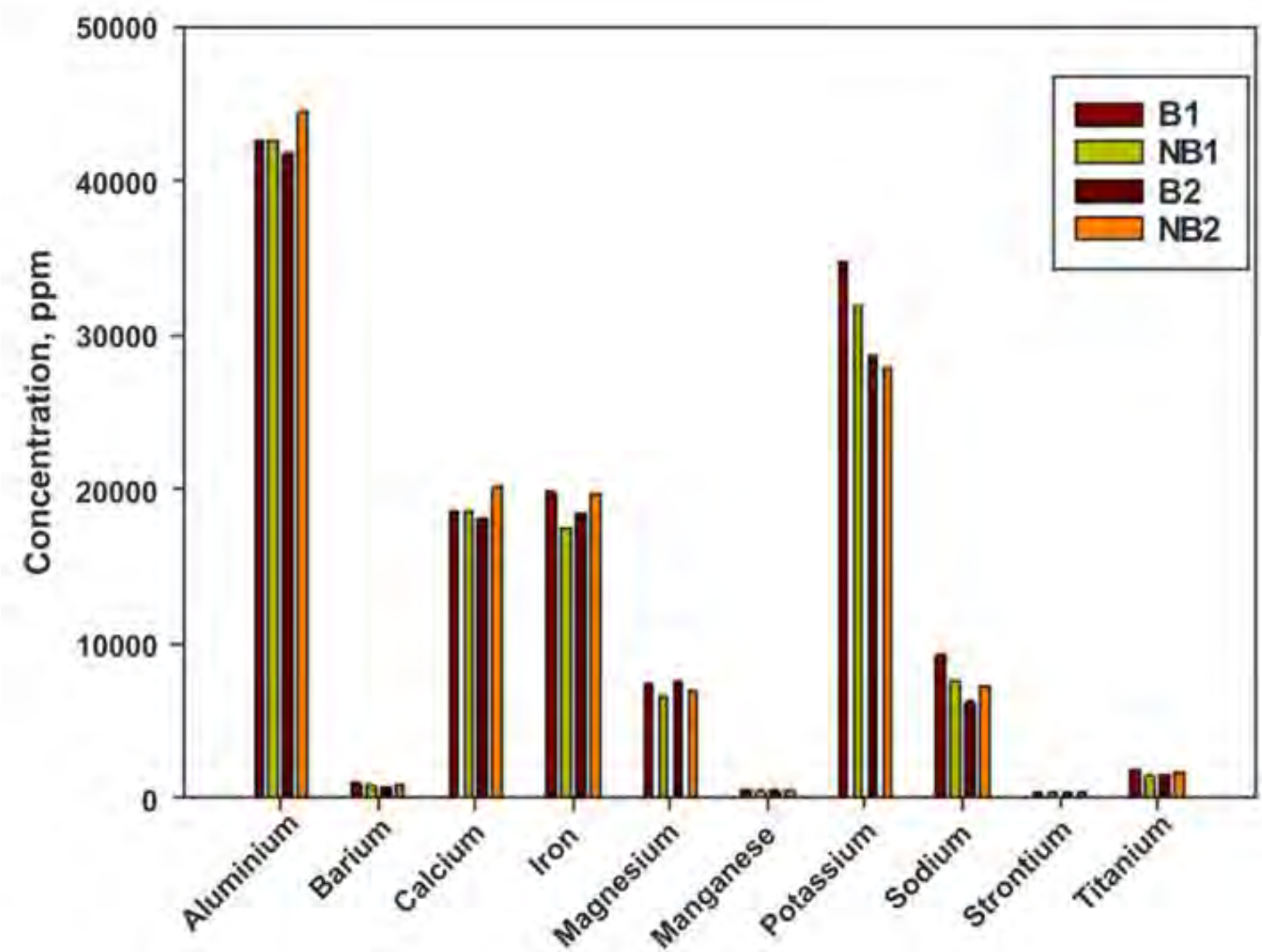

Figure_13
Click here to download high resolution image

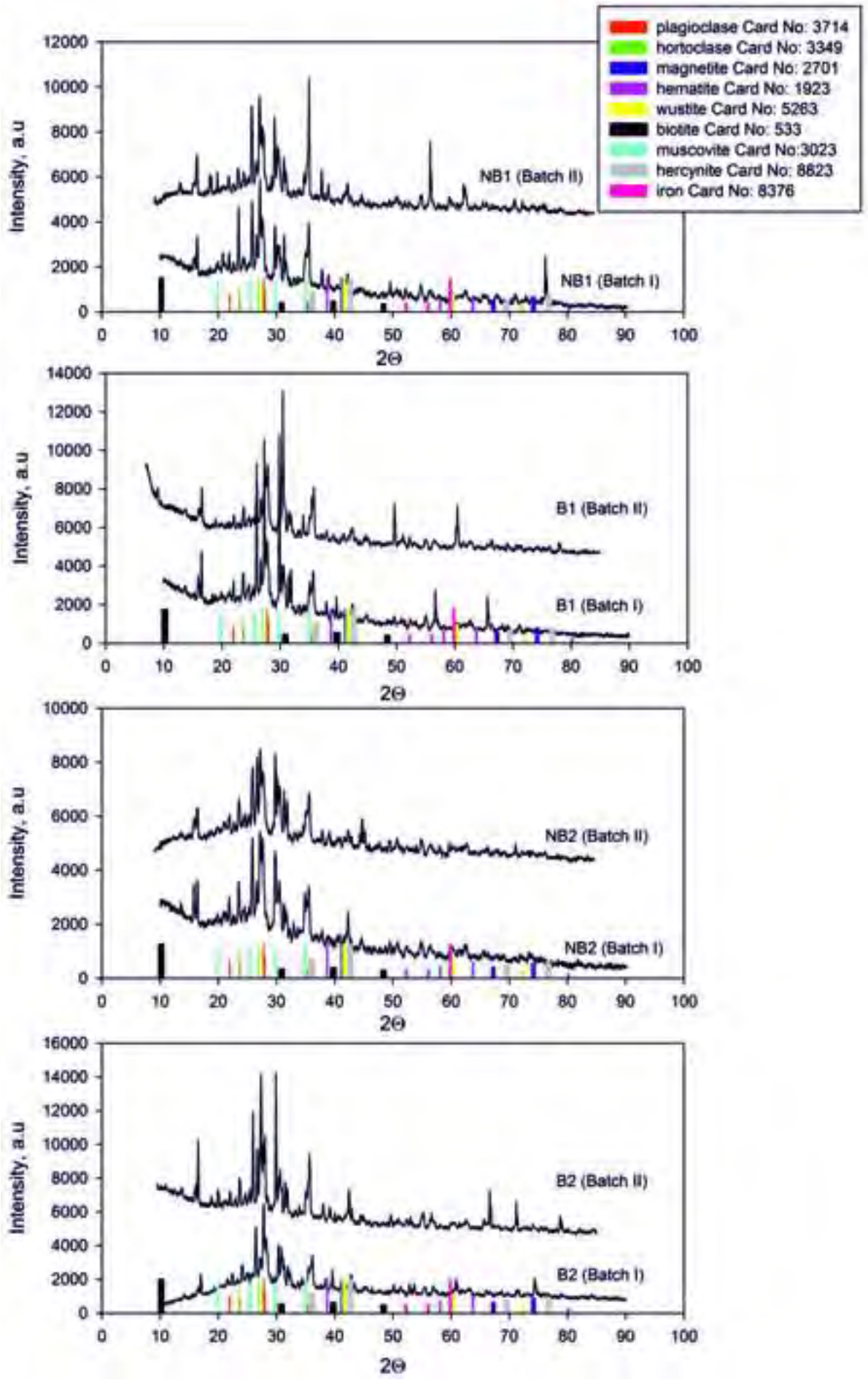

Figure_14

Click here to download high resolution image

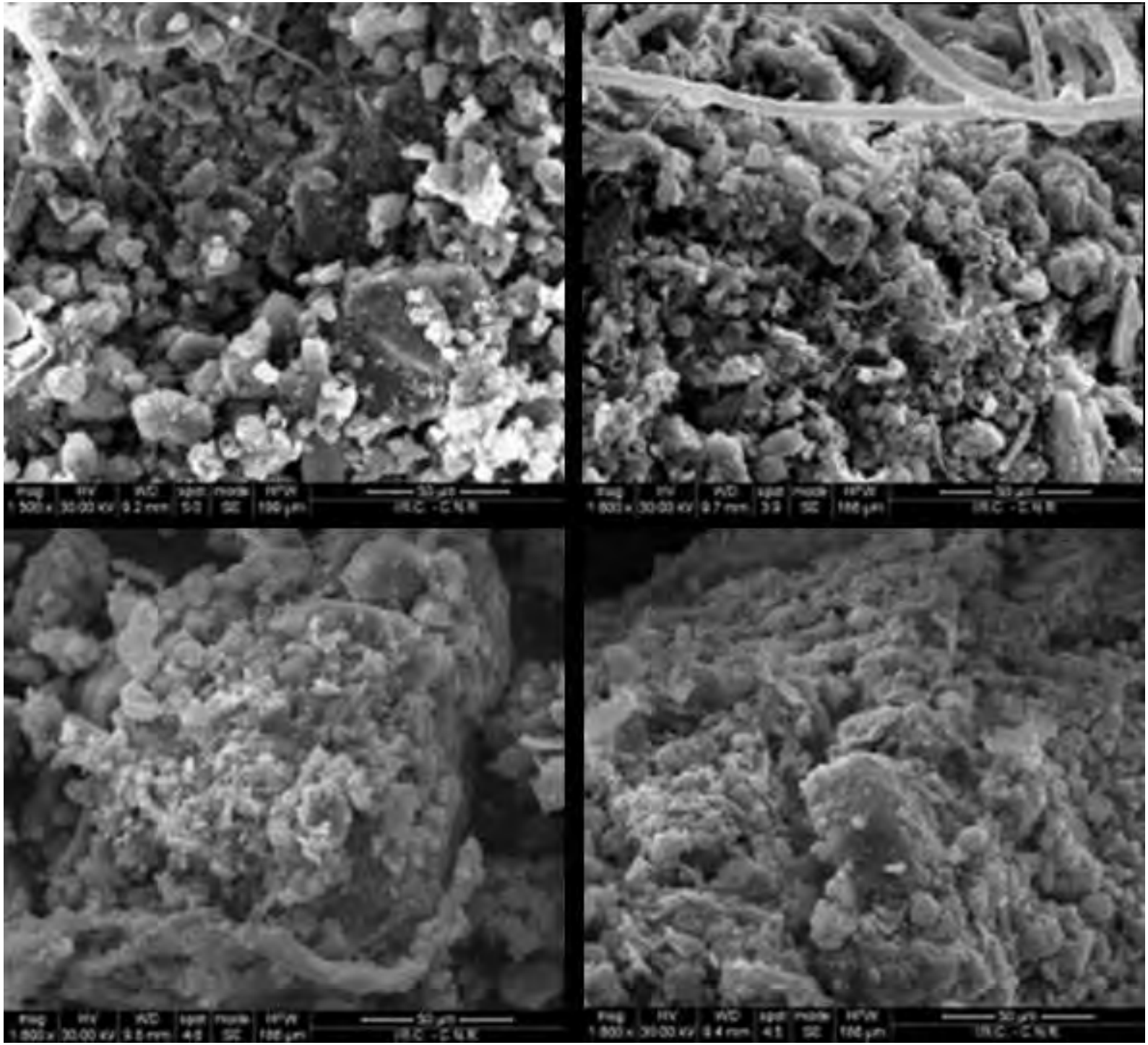

FIGURE 1 (color in print)

Figure 1. A) Location of the study area; the Campania region is highlighted in black. B) Geological sketch-map of the Sarno Mountain Range and the surrounding area (ISPRA, 1976).

FIGURE 2 (color on the web only)

Figure 2. Slope map (on the left) and pyroclastic cover thickness map (on the right) of the Sant'Angelo Creek watershed (Autorità di Bacino del Sarno, 2011 modified). Map coordinate system: UTM 33N - WGS84.

FIGURE 3 (color on the web only)

Figure 3. Soil burn severity map of the Sant'Angelo Creek fire including location of the collected samples and WDPT tests. Map coordinate system: UTM 33N - WGS84.

FIGURE 4 (color on the web only)

Figure 4. Daily rainfall depth and related peak 10-minute rainfall intensity (I_{10}) recorded by the "Cetronico" rain gauge in the period 1 August - 10 September, 2012. The occurrence of the Sant'Angelo Creek fire (dashed line) and the 06.09.2012 post-fire erosion response (black arrow) are highlighted.

FIGURE 5 (color on the web only)

Figure 5. The 6 September, 2012 rainfall recorded by the Cetronico rain gauge. The inset shows both cumulative rainfall profile and rainfall intensity profile measured from the beginning (minute 0 = 04.50 hrs) until the end (minute 100 = 6.30 hrs) of the rainstorm.

FIGURE 6 (color on the web only)

Figure 6. A picture of the unburned part of the Sant'Angelo creek watershed. It highlights as the soil surface is protected by a thick vegetation cover.

FIGURE 7 (color on the web only)

Figure 7. Evidences of erosion by surface runoff. A) Light band formed by the overland flows which removed a soil patch from the base of a trunk located along the runoff path; B) Bare roots associated with a light band.

FIGURE 8 (color on the web only)

Figure 8. Rill network developing in the topsoil of the area burned with high soil burn severity.

FIGURE 9 (color in print)

Figure 9. Soil erosion intensity map. The inset shows a 3D scheme of the concrete channel partially filled by sediments and closed by a sealed culvert as well as a real picture of the channel captured during the field survey.

FIGURE 10 (color on the web only)

Figure 10. Evidence of soil redistribution processes. Burned material (leafs, ashes, mineral soil particles) accumulated by the overland flows in the back side of a trunk. The leafs show an embricated structure related to the overland flow direction (yellow arrow).

FIGURE 11 (color on the web only)

Figure 11. Cumulative curves of the particle size distribution related to the samples collected in the study area, overlapped by those of Meyer and Wells (1997) delimiting the flow faces fields (dashed black lines). The solid lines of deposit samples D1 and D2 fall in the hyperconcentrated flow and streamflow fields, respectively.

FIGURE 12 (color on the web only)

Figure 12. Inorganic elemental analysis of burned and unburned soil samples.

FIGURE 13 (color in print)

Figure 13. XRD spectra of burned and unburned soil samples.

FIGURE 14 (color on the web only)

Figure 14. SEM images of NB1 (top left), NB2 (top right), B1 (bottom left) and B2 (bottom right) samples.

Interactive Map file (.kml or .kmz)

Click here to download Interactive Map file (.kml or .kmz): santangelo creek fire.kml